

Medium effects in cooling of neutron stars and the $3P_2$ neutron gap

H. Grigorian^{1,2} and D. N. Voskresensky^{3,4}

¹ Institut für Physik, Universität Rostock, Universitätsplatz 3, 18051 Rostock, Germany
e-mail: hovik.grigorian@uni-rostock.de

² Department of Physics, Yerevan State University, Alex Manoogian Str. 1, 375025 Yerevan, Armenia

³ Gesellschaft für Schwerionenforschung mbH, Planckstr. 1, 64291 Darmstadt, Germany
e-mail: d.voskresensky@gsi.de

⁴ Moscow Institute for Physics and Engineering, Kashirskoe sh. 31, 115409 Moscow, Russia

Received 31 January 2005 / Accepted 2 August 2005

ABSTRACT

We study the dependence of the cooling of isolated neutron stars on the magnitude of the $3P_2$ neutron gap. Our “nuclear medium cooling” scenario favors a suppressed value of the $3P_2$ neutron gap.

Key words. dense matter – neutrinos – nuclear reactions, nucleosynthesis, abundances – ISM: evolution

1. Introduction

Theoretical study of neutron star (NS) cooling began with pioneering works of Tsuruta & Cameron (1965) and Bahcall & Wolf (1965). It has been argued that one-nucleon direct Urca (DU) processes $n \rightarrow pe\bar{\nu}$, $pe \rightarrow nv$ are forbidden up to sufficiently high density and the main role is played by the two-nucleon modified Urca (MU) processes, like $nm \rightarrow npe\bar{\nu}$ and $np \rightarrow ppe\bar{\nu}$. The “standard” scenario of NS cooling emerged, where the main process responsible for the cooling is the modified Urca process MU $nm \rightarrow npe\bar{\nu}$ calculated using free one pion exchange (FOPE) between nucleons, see Friman & Maxwell (1979). An order of magnitude less contribution to the neutrino emissivity is given by the nucleon bremsstrahlung (NB) processes. The main process among NB processes responsible for the cooling is neutron-neutron bremsstrahlung $nn \rightarrow nn\nu\bar{\nu}$, neutron-proton bremsstrahlung $pn \rightarrow pnv\bar{\nu}$ is less effective, and the proton-proton one $pp \rightarrow pp\nu\bar{\nu}$ is even less effective. This scenario explains only the group of slow cooling data. To explain the group of rapidly cooling data the “standard” scenario was supplemented by “exotic” processes either with a pion condensate, with a kaon condensate, with hyperons, or involving DU reactions, see Tsuruta (1979), Shapiro & Teukolsky (1983) and references therein. All these processes may occur only for densities higher than a critical density, $(2 \div 6) n_0$, depending on the model, where n_0 is the nuclear saturation density.

Pair breaking and formation (PBF) processes permitted in nucleon superfluids have been suggested. Flowers et al. (1976)

calculated the emissivity of $1S_0$ neutron pair breaking and formation (nPBF) process and Voskresensky & Senatorov (1987) considered the general case. Neutron and proton pair breaking and formation processes (pPBF) were incorporated within a closed diagram technique including medium effects. Numerical estimates are valid both for $1S_0$ and $3P_2$ superfluids. Schaab et al. (1997) have shown that the inclusion of PBF processes into the cooling code may allow one to describe the “intermediate cooling” group of data (even if one artificially suppresses the effects of the medium). Thus the “intermediate cooling” scenario arose.

The PBF processes were then incorporated in the cooling codes of other groups, that worked with the “standard plus exotics” scenario, see Tsuruta et al. (2002), Yakovlev et al. (2004a), Page et al. (2004). Recently Page et al. (2004) called the approach that incorporates the PBF processes into the “standard” scenario, the “minimal cooling” paradigm. Some papers included the possibility of internal heating that results in a slowing down of the cooling of old pulsars, see Tsuruta (2004) and refs. therein. However, because of the simplification of the consideration, calculations within the “standard plus exotics” scenario or within the “minimal cooling” paradigm did not incorporate effects of the medium.

The necessity to include in-medium effects in the NS cooling problem is a rather obvious issue. It is based on requirements of condensed matter physics, of the physics of the atomic nucleus and heavy ion collisions, see Migdal et al. (1990) Rapp & Wambach (1994), Ivanov et al. (2001). The relevance of in-medium effects for the NS cooling problem has been shown

by Voskresensky & Senatorov (1984, 1986, 1987), Senatorov & Voskresensky (1987), Migdal et al. (1990), Voskresensky (2001) who calculated emissivity of the MU, NB and PFB processes taking into account in-medium effects. We call these processes medium-modified Urca process (MMU), medium nucleon bremsstrahlung (MNB) and medium pair breaking and formation (MPBF) processes. The efficiency of the developed “nuclear medium cooling” scenario for the description of NS cooling was demonstrated within the cooling code by Schaab et al. (1997) and then by Blaschke et al. (2004). In the latter paper it was shown that it is possible to fit the whole set of cooling data available today. Besides the incorporation of in-medium effects into the pion propagator and the vertices, it was also exploited that the $3P_2$ neutron gaps are dramatically suppressed. The latter assumption was motivated by the analysis of the data (see Figs. 12, 15, 20–23 of Blaschke et al. 2004) and by recent calculations of the $3P_2$ neutron gaps by Schwenk & Friman (2004). However more recent work of Khodel et al. (2004) suggested that the $3P_2$ neutron pairing gap should be dramatically enhanced, as a consequence of the strong softening of the pion propagator. Thus the results of calculations of Schwenk & Friman (2004) and Khodel et al. (2004), which both aim to include medium effects in the evaluation of the $3P_2$ neutron gaps, are contradictory.

Our aim here is to check the consequences of an enhanced $3P_2$ neutron pairing gap within the “nuclear medium cooling” scenario following the work of Blaschke et al. (2004). The paper is organized as follows. In Sect. 2 we start with a brief recapitulation of the Landau-Migdal Fermi liquid approach. Section 2.1 calculates the NN interaction amplitude. In Sect. 2.2 we separate the in-medium pion mode yielding the main contribution to the NN interaction for $n > n_0$. Section 2.3 demonstrates the importance of the renormalization of the weak interaction in the medium. In Sect. 2.4 we show internal inconsistencies of the FOPE model, which is the basis of the “standard” scenario. Then in Sect. 3 we recapitulate the main processes as they are treated within the “nuclear medium cooling” scenario. In Sect. 4 we discuss calculations of the pairing gaps and how gaps affect the emissivities of different processes. Then in Sect. 5.1 we discuss the cooling model of Blaschke et al. (2004). In Sect. 6 we present emissivities of the main processes, the heat capacity and thermal conductivity contributions in the scenario of Khodel et al. (2004), when the neutron processes are assumed to be frozen. In Sect. 7 we show our numerical results. Concluding remarks are given in Sect. 8.

2. Medium effects. Nuclear Fermi liquid

2.1. NN interaction. Hard and soft modes

At temperatures of interest ($T \ll \varepsilon_{Fn}, \varepsilon_{Fp}$) neutrons and even protons are only slightly excited above their Fermi seas and all the processes occur in the close vicinity of the Fermi energies $\varepsilon_{Fn}, \varepsilon_{Fp}$. Quasiparticle approximation is fulfilled for nucleons. In such a situation a Fermi liquid approach seems to be the most efficient one. Within this approach the long-scale phenomena are treated explicitly whereas short-scale ones are described by the local quantities expressed via phenomenological

Landau-Migdal parameters. We deal with the baryon densities $7n_0 \gtrsim n \gtrsim 0.5n_0$. The value $n_0 \approx 0.5m_\pi^3$, where $m_\pi = 140$ MeV is the pion mass, $\hbar = c = 1$. At such densities related to inter-nucleon distances $d \sim 1/n^{1/3} \sim (0.5 \div 1.3) 1/m_\pi$ processes important for the description of the NN interaction correspond to typical energies and momenta $\omega, k \lesssim$ few m_π . We call them the long-range processes and treat them explicitly. These are nucleon particle-hole processes, Δ isobar-nucleon hole processes (since the typical energy of the isobar is of the order of the mass difference $m_\Delta - m_N \approx 2.1 m_\pi$) and processes related to the excitation of the pion (the typical excitation energy is of the order of the pion mass). Thus we explicitly present loop diagrams which depend strongly on the energy and momentum for the $\omega, k \lesssim$ few m_π of our interest.

Using the above argumentation of Fermi liquid theory (see Landau 1956; Migdal 1967; Migdal et al. 1990) the retarded NN interaction amplitude is presented as follows (see also Voskresensky 2001, for further details)

Diagrammatic equation (1) shows a four-point vertex (left) equal to the sum of two diagrams (right). The first diagram on the right is a particle-hole diagram with a shaded circle and a solid line. The second diagram is a delta-nucleon hole diagram with a shaded circle and a double-line. There are two such diagrams on the right, one above the other, separated by a plus sign.

where

Diagrammatic equation (2) shows a shaded circle (left) equal to the sum of two diagrams (right). The first diagram is a particle-hole diagram with a shaded circle and a solid line. The second diagram is a double-wave line diagram with two wavy lines.

The solid line presents the quasiparticle Green function of the nucleon, the double-line is that of the Δ isobar¹. Thus most long-range diagrams of the particle-hole and Δ -nucleon hole types are explicitly presented in (1). Other long-range terms come from the pion. The double-wave line in (2) corresponds to the exchange of the free pion with inclusion of the contributions of the residual S wave πNN interaction and $\pi\pi$ scattering, i.e. the residual interaction irreducible to the nucleon particle-hole and delta-nucleon hole. The latter contributions we have taken into account in (1). Thus the full particle-hole, delta-nucleon hole and pion irreducible block (first block in (2)) is by its construction significantly more local than contributions given by explicitly presented graphs. If we decided to calculate the irreducible block in (2) we would need to introduce σ, ω, ρ exchanges and to treat diagrams with multiple pion lines. All these terms are less energy-momentum dependent for $\omega, k \lesssim$ few m_π than those we treat explicitly.

Up to now we have not perform any approximations, except the quasiparticle approximation for the nucleons. Now we perform the main approximation. Using the locality argument, one assumes that the Landau-Migdal parameters, f_{nn}, f_{np} in the scalar channel and g_{nn}, g_{np} in the spin channel, which parameterize the first block in (2), are approximately constant. Their values are extracted from analysis of experimental data. In a

¹ Diagrams with open particle lines have sense only if the quasiparticle approximation is valid. Otherwise one needs to use the closed diagram technique developed by Voskresensky & Senatorov (1987), Knoll & Voskresensky (1995, 1996).

more extended approach these parameters should certainly be calculated as functions of the density, neutron and proton concentrations, energy and momentum.

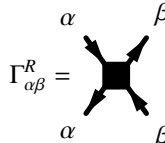
The part of interaction involving Δ isobar is analogously constructed



$$\text{[Diagram]} = \text{[Diagram]} + \text{[Diagram]} \quad (3)$$

The main part of the $N\Delta$ interaction is due to the pion exchange. Although information on the local part of the $N\Delta$ interaction is rather scarce, one can conclude (Migdal et al. 1990; Suzuki et al. 1999) that the corresponding Landau-Migdal parameters are essentially smaller than those for the NN interaction. Therefore for simplicity we neglect the first graph in the r.h.s. of (3).

Straightforward resummation of (1) in the neutral channel yields (Voskresensky & Senatorov 1987; Migdal et al. 1990)



$$\Gamma_{\alpha\beta}^R = C_0 (\mathcal{F}_{\alpha\beta}^R + \mathcal{Z}_{\alpha\beta}^R \sigma_1 \cdot \sigma_2) + f_{\pi N}^2 \mathcal{T}_{\alpha\beta}^R (\sigma_1 \cdot \mathbf{k})(\sigma_2 \cdot \mathbf{k}), \quad (4)$$

$$\mathcal{F}_{\alpha\beta}^R = f_{\alpha\beta} \gamma(f_{\alpha\beta}), \quad \mathcal{Z}_{mn}^R = g_{mn} \gamma(g_{mn}), \quad (5)$$

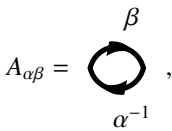
$$\mathcal{Z}_{np}^R = g_{np} \gamma(g_{np}), \quad \alpha, \beta = (n, p),$$

$$\mathcal{T}_{mn}^R = \gamma^2(g_{mn}) D_{\pi^0}^R, \quad \mathcal{T}_{np}^R = -\gamma_{pp} \gamma(g_{mn}) D_{\pi^0}^R,$$

$$\mathcal{T}_{pp}^R = \gamma_{pp}^2 D_{\pi^0}^R,$$

$$\gamma^{-1}(x) = 1 - 2x C_0 A_{nn}^R, \quad \gamma_{pp} = (1 - 4g C_0 A_{nn}^R) \gamma(g_{nn}),$$

$f_{nn} = f_{pp} = f + f'$, $f_{np} = f - f'$, $g_{nn} = g_{pp} = g + g'$, and $g_{np} = g - g'$, the dimensional normalization factor is usually taken to be $C_0 = \pi^2 / [m_N p_{FN}(n_0)] \simeq 300 \text{ MeV fm}^3 \simeq 0.77 m_\pi^{-2}$, $p_{FN}(n_0)$ is the nucleon Fermi momentum in the atomic nucleus, $D_{\pi^0}^R$ is the full retarded Green function of π^0 , $A_{\alpha\beta}$ is the corresponding NN^{-1} loop (without spin degeneracy factor 2)

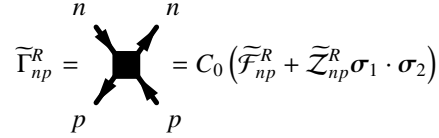


$$A_{\alpha\beta} = \frac{\text{[Diagram]}}{\alpha^{-1}}, \quad (6)$$

$$A_{nn}(\omega \simeq q) \simeq m_n^{*2} (4\pi^2)^{-1} \left(\ln \frac{1 + v_{Fn}}{1 - v_{Fn}} - 2v_{Fn} \right),$$

$A_{nn} \simeq -m_n^* p_{FN} (2\pi^2)^{-1}$, for $\omega \ll q v_{Fn}$, $q \ll 2p_{FN}$, $p_{FN} = m_n^* v_{Fn}$, m_n^* is the effective neutron mass in medium, and for simplicity we neglect proton hole contributions due to the low concentration of protons. The term proportional to C_0 in (4) demonstrates the change of the local block by the long-range loop NN correlation factors and the term proportional to the pion-nucleon coupling constant $f_{\pi N}$ demonstrates the change of the second (pion) term in (2).

Resummation of (1) in the charged channel yields



$$\Gamma_{np}^R = C_0 (\tilde{\mathcal{F}}_{np}^R + \tilde{\mathcal{Z}}_{np}^R \sigma_1 \cdot \sigma_2) + f_{\pi N}^2 \tilde{\mathcal{T}}_{np}^R (\sigma_1 \cdot \mathbf{k})(\sigma_2 \cdot \mathbf{k}), \quad (7)$$

$$\tilde{\mathcal{F}}_{np}^R = 2f' \tilde{\gamma}(f'), \quad \tilde{\mathcal{Z}}_{np}^R = 2g' \tilde{\gamma}(g'),$$

$$\tilde{\mathcal{T}}_{np}^R = \tilde{\gamma}^2(g') D_{\pi^-}^R, \quad (8)$$

$$\tilde{\gamma}^{-1}(x) = 1 - 4x C_0 A_{np}^R,$$

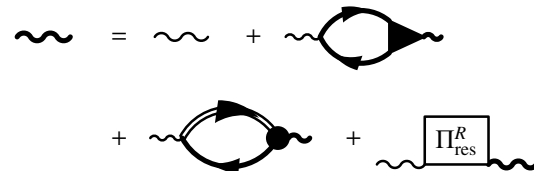
$D_{\pi^-}^R$ is the full retarded Green function of π^- . The Landau-Migdal parameters are poorly known for isospin asymmetric nuclear matter and for $n > n_0$. Taking into account the arguments that they can be considered approximately as constants, for estimates we may use the values extracted from atomic nucleus experiments. One can expect that the most uncertain will be the value of the scalar constant f due to the essential role of the medium-heavy σ meson in this channel. But this parameter does not enter the tensor force channel which is the most important in our case. Unfortunately, there are also uncertainties in the numerical values of the Landau-Migdal parameters in other channels and even for atomic nuclei. These uncertainties are, mainly, due to attempts to get the best fit of experimental data in each concrete case, slightly modifying the parameterization used for the residual part of the NN interaction. For example, calculations by Migdal (1967) gave $f \simeq 0.25$, $f' \simeq 1$, $g \simeq 0.5$, $g' \simeq 1$ whereas Saperstein & Tolokonnikov (1998), Fayans & Zawischa (1995), Borzov et al. (1984), including quasiparticle renormalization pre-factors, derived the values $f \simeq 0$, $f' \simeq 0.5 \div 0.6$, $g \simeq 0.05 \pm 0.1$, $g' \simeq 1.1 \pm 0.1$.

Typical energies and momenta entering the NN interaction amplitude of interest are $\omega \simeq 0$ and $k \simeq p_{FN}$. Then one estimates $\gamma(g_{nn}, \omega \simeq 0, k \simeq p_{FN}, n = n_0) \simeq 0.35 \div 0.45$. For $\omega = k \simeq T$ typical for the weak processes with $\nu\bar{\nu}$ one has $\gamma^{-1}(g_{nn}, \omega \simeq k \simeq T, n = n_0) \simeq 0.8 \div 0.9$.

2.2. Virtual pion mode

The pion is strongly affected by the nucleon surroundings. It is obvious already from the fact that typical densities are $n \sim 1$ and the pion-nucleon coupling constant is $f_{\pi N} = 1$ in units $m_\pi = \hbar = c = 1$. Obviously perturbation theory is not applicable in this case. Instead we continue to use the Fermi liquid approach suitable for the description of the strong interaction.


A straightforward resummation of diagrams (1), (2) yields the following re-summed Dyson equation for pions



$$\text{[Diagram]} = \text{[Diagram]} + \text{[Diagram]} + \text{[Diagram]} + \text{[Diagram]} \quad (9)$$

The $\pi N\Delta$ full-dot-vertex includes a phenomenological background correction due to the presence of the higher resonances, Π_{res}^R is the residual retarded pion self-energy that includes the contribution of all the diagrams which are not presented explicitly in (9), such as S wave πNN and $\pi\pi$ scatterings (included by double-wavy line in (2)). For zero temperature the main contribution to Π_{res}^R is given by the Weinberg-Tomozawa term which has a simple analytic form. A part of Π_{res}^R related to $\pi\pi$ fluctuations is important for the description of the vicinity of the pion condensation critical point. It is calculated explicitly. Other contributions are rather small and can be neglected, as follows from the comparison of the theory predictions with different atomic nucleus data, see Migdal et al. (1990).

The full πNN vertex takes into account NN correlations




$$\text{Full } \pi NN \text{ vertex} = \text{Single } \pi \text{ exchange} + \text{Pion exchange with } NN \text{ correlation} \quad (10)$$

Therefore the nucleon particle-hole part of Π_{π^0} is $\propto \gamma(g_{nn})$ and the nucleon particle-hole part of Π_{π^\pm} is $\propto \gamma(g')$. The value of the NN interaction in the pion channel is determined by the full pion propagator at small ω and $k \simeq p_{Fn}$, i.e. by the quantity

$$(\omega^*)^2(k) = -(D_\pi^R)^{-1}(\omega = 0, k, \mu_\pi). \quad (11)$$

Typical momenta of interest are $k \simeq p_{Fn}$. Indeed the momenta entering the NN interaction in MU and MMU processes are $k = p_{Fn}$, the momenta governing the MNB are $k = k_m$ (Voskresensky & Senatorov 1986) where the value $k = k_m \simeq (0.9 \div 1)p_{Fn}$ corresponds to the minimum of $(\omega^*)^2(k)$. The quantity $\omega^* \equiv \omega^*(k_m)$ is the *effective pion gap*, i.e., the effective pion mass in some sense. The effective pion gap ω^* demonstrates how much the virtual (particle-hole) mode with pion quantum numbers is softened at a given density. The quantity $\omega^{*2}(p_{Fn}(n))$ replaces the value $(m_\pi^2 + p_{Fn}^2)$ in the case of the free pion propagator used for the calculation of the MU process by Friman & Maxwell (1979). It is different for π^0 and for π^\pm since neutral and charged channels are characterized by different diagrams permitted by charge conservation, thus also depending on the value of the pion chemical potential, $\mu_{\pi^+} \neq \mu_{\pi^-} \neq 0$, $\mu_{\pi^0} = 0$. For $T \ll \varepsilon_{Fn}, \varepsilon_{Fp}$, one has $\mu_{\pi^-} = \mu_e = \varepsilon_{Fn} - \varepsilon_{Fp}$, as follows from equilibrium conditions for the reactions $n \rightarrow p\pi^-$ and $n \rightarrow p\bar{\nu}$.

As follows from numerical estimates of different γ factors entering (4) and (7), the main contribution to NN interaction for $n > n_0$ is given by the resummed medium one pion exchange (MOPE) diagram



$$\text{MOPE diagram} \simeq \text{Resummed MOPE diagram} \quad (12)$$

if this channel ($\mathcal{T} \propto (\sigma_1 \cdot k)(\sigma_2 \cdot k)$, see (7), (4)) of the reaction is not forbidden or suppressed by specific effects such as symmetry, small momentum transfer, etc.

The density dependence of the effective pion gap ω^* that we use in this work is demonstrated in Fig. 1 (Fig. 1 of Blaschke et al. 2004). The curve 1a in Fig. 1 shows the behavior of the pion gap for $n < n_c^{\text{PU}}$, where n_c^{PU} is the critical density for the

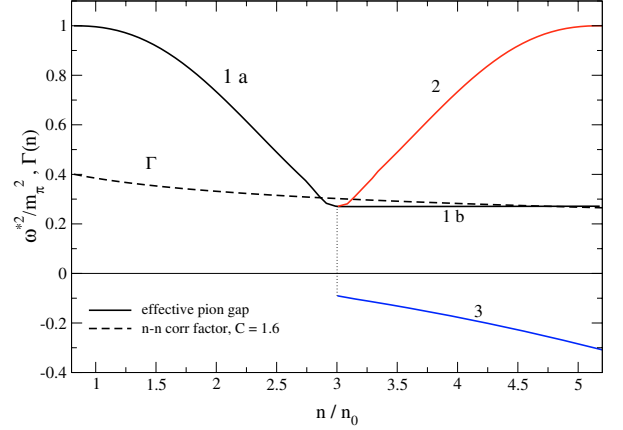


Fig. 1. Nucleon–nucleon correlation factor Γ and square of the effective pion gap ω^* with pion condensation (branches 1a, 2, 3) and without (1a, 1b).

pion condensation. In this work for simplicity we do not distinguish between different possibilities of π^0 , π^\pm condensations and the so-called alternative-layer-structure, see Voskresensky & Senatorov (1984), Migdal et al. (1990) and Umeda et al. (1994). Thus we assume that π^0 and π^- condensations occur at the very same critical density n_c^{PU} . Although the value n_c^{PU} depends on rather uncertain different parameters we, following Blaschke et al. (2004), further assume $n_c^{\text{PU}} \simeq 3 n_0$, cf. discussion by Migdal et al. (1990). The curve 1b demonstrates the possibility of a saturation of pion softening and the absence of pion condensation for $n > n_c^{\text{PU}}$ (this possibility could be realized, e.g., if Landau-Migdal parameters increased with the density). This pion gap (from curves 1a+1b) is the value that determines the pion Green function for the pion excitations. Curves 2, 3 demonstrate the possibility of pion condensation for $n > n_c^{\text{PU}}$. The continuation of branch 1a for $n > n_c^{\text{PU}}$, called branch 2, shows the reconstruction of the pion dispersion relation in the presence of the condensate state. This pion gap is the value that determines the pion Green function for the pion excitations above the pion condensate vacuum. In the presence of the pion condensate (for $n > n_{c\pi}$) the value ω^* from curve 2 enters the emissivities of all processes with pion excitations in initial, intermediate and final reaction states.

In agreement with the general trend known in condensed matter physics, fluctuations dominate in the vicinity of the critical point of the phase transition and die out far away from it. The jump from branch 1a to 3 at $n = n_c^{\text{PU}}$ is due to the first order phase transition to the π condensation, see discussion of this point by Dyugaev (1975, 1982), Voskresensky & Mishustin (1981, 1982), Migdal et al. (1990). The $|\omega^*|$ value on branch 3 is proportional to the amplitude of the pion condensate mean field (the line with the cross in the standard notation of the diagram technique).

The observation that pion condensation appears by the first order phase transition needs a comment. The first order phase transitions in the systems with several charged species is associated with the possibility of a mixed phase, see Glendenning (1992). The emissivity is increased within the mixed phase since efficient DU-like processes due to nucleon re-scattering

on the new-phase droplets are possible. However Voskresensky et al. (2002, 2003) and Maruyama et al. (2003, 2005a) demonstrated that, if it exists, the mixed phase is probably realized only in a narrow density interval due to charge screening effects. Thereby to simplify the consideration we further disregard the possibility of a mixed phase. We also disregard the change in the equation of state (EoS) due to pion condensation assuming that the phase transition is rather weak.

The density dependence of the correlation factor Γ is presented in Fig. 1. For the correlation factor entering the emissivity of the MMU process one can use an approximate expression $\Gamma(n) \approx 1/[1 + C(n/n_0)^{1/3}]$, $C \approx 1.4 \div 1.6$. Note that this value Γ is an averaged quantity ($\Gamma^6 = \Gamma_{w-s}^2 \Gamma_s^4$). Actually the correlation factor Γ^6 entering the emissivity of the MMU process (see Eq. (23) below) looks more involved and depends on the energy-momentum transfer, being different for vertices connected to the weak coupling (the correlation factor related to the weak coupling vertices Γ_{w-s} is close to unity) and for vertices related to the pure strong coupling (Γ_s is slightly less than above introduced factor Γ), see estimates of the energy-momentum dependence of the correlation factors at the end of the previous subsection. We see that vertices are rather strongly suppressed (and this suppression increases with the density) but the softening of the pion mode is enhanced ($\omega^{*2} < m_\pi^2$) for $n > n_{c1} \approx 0.5 \div 0.8 n_0$. Such a behavior is supported both theoretically and by analysis of nuclear experiments, see Migdal et al. (1990).

Even with full microscopic calculations the functions $\Gamma(n)$ and $\omega^*(n)$ contain large uncertainties. These uncertainties come mainly from simplifications inherent to the Landau-Migdal approach to nuclear forces where the Landau-Migdal parameters are constants. However it seems misleading to disregard medium effects only based on existing rather large uncertainties. We believe that further more detailed comparison of theory and experiment will allow one to reduce these uncertainties.

2.3. Renormalization of the weak interaction.

The full weak coupling vertex that takes into account NN correlations is determined by (10) where now the wavy line should be replaced by the lepton pair. Thus for the vertex of interest, $N_1 \rightarrow N_2 l \bar{\nu}$, we obtain, see Voskresensky & Senatorov (1987), Migdal et al. (1990),

$$V_\beta = \frac{G}{\sqrt{2}} [\tilde{\gamma}(f') l_0 - g_A \tilde{\gamma}(g') l \sigma], \quad (13)$$

for the β decay and

$$V_{nn} = -\frac{G}{2\sqrt{2}} [\gamma(f_{nn}) l_0 - g_A \gamma(g_{nn}) l \sigma],$$

$$V_{pp}^N = \frac{G}{2\sqrt{2}} [\kappa_{pp} l_0 - g_A \gamma_{pp} l \sigma], \quad (14)$$

$$\kappa_{pp} = c_V - 2f_{np} \gamma(f_{nn}) C_0 A_{nn},$$

$$\gamma_{pp} = (1 - 4g C_0 A_{nn}) \gamma(g_{nn}), \quad (15)$$

for processes on the neutral currents $N_1 N_2 \rightarrow N_1 N_2 \nu \bar{\nu}$, $V_{pp} = V_{pp}^N + V_{pp}^\gamma$, $G \approx 1.17 \times 10^{-5} \text{ GeV}^{-2}$ is the Fermi weak coupling

constant, $c_V = 1 - 4 \sin^2 \theta_W$, $\sin^2 \theta_W \approx 0.23$, $g_A \approx 1.26$ is the axial-vector coupling constant, and $l_\mu = \bar{u}(q_1) \gamma_\mu (1 - \gamma_5) u(q_2)$ is the lepton current. The pion contribution $\sim q^2$ is small for typical $|q| \approx T$ or p_{Fe} , and for simplicity is omitted. In medium the value of g_A (i.e. g_A^*) slightly decreases with the density.

The γ factors renormalize the corresponding vacuum vertices. These factors are different for different processes. The matrix elements of the neutrino/antineutrino scattering processes $N\nu \rightarrow N\nu$ and of MNB behave differently depending on the energy-momentum transfer and whether $N = n$ or $N = p$ in the weak coupling vertex. Vertices

$$\text{Diagram 1: } \nu \text{ and } \bar{\nu} \text{ lines meeting at a vertex connected to an } N \text{ line.} \quad \text{Diagram 2: } \nu \text{ and } \bar{\nu} \text{ lines meeting at a vertex connected to two } N \text{ lines.} \quad (16)$$

are modified by the correlation factors (5) and (8). For $N = n$ these are $\gamma(g_{nn}, \omega, q)$ and $\gamma(f_{nn}, \omega, q)$ leading to an enhancement of the cross sections for $\omega > qv_{Fn}$ and to a suppression for $\omega < qv_{Fn}$.

Renormalization of the proton vertex (vector part of $V_{pp}^N + V_{pp}^\gamma$) is governed by the processes, see Voskresensky & Senatorov (1987), Voskresensky et al. (1998),

$$\text{Diagram 1: } p \text{ line with } n \text{ loop and } n^{-1} \text{ line, connected to } \nu \text{ and } \bar{\nu}. \quad \text{Diagram 2: } p \text{ line with } e \text{ loop and } p \text{ line, connected to } \nu \text{ and } \bar{\nu}. \quad (17)$$

being forbidden in vacuum but permitted in medium. For the systems with $1S_0$ proton–proton pairing, $\propto g_A^2$ contribution to the squared matrix element (see (14)) is compensated by the corresponding contribution of the diagram with anomalous Green functions of protons. The vector current term is $\propto c_V^2$ in vacuum whereas it is $\propto \kappa_{pp}^2$ in medium (by the first diagram in (17)). Thereby the corresponding vertices with protons are enhanced in medium compared to small vacuum values ($\propto c_V^2 \approx 0.006$) leading to enhancement of the cross sections, up to $\sim 10 \div 10^2$ times for $1.5 \div 3n_0$ depending on the choice of the parameters. It does not contradict the statement that correlations are suppressed in the weak interaction vertices at $n \leq n_0$. Enhancement with density comes from estimation (6) (that directly follows from Eq. (2.30) of Voskresensky & Senatorov 1987). Also as enhancement factor (up to $\sim 10^2$) comes from the virtual in-medium photon (γ_m), second diagram in (17), whose propagator contains $1/m_\gamma^2 \sim 1/e^2$, where m_γ is the effective spectrum gap, that compensates for the small e^2 factor from electromagnetic vertices, see Voskresensky et al. (1998),

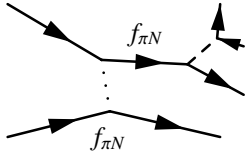
Leinson (2000). It is included by replacing $V_{pp}^N \rightarrow V_{pp}$. Other processes permitted in intermediate states like processes with pp^{-1} and with pions are suppressed by a low proton density and by $q^2 \sim T^2$ pre-factors, respectively. The first diagram in (17) was considered in Voskresensky & Senatorov (1987), where the MpPBF process was first introduced, and then in Migdal et al. (1990), Schaab et al. (1997), and it was shown that MnPBF and MpPBF processes may give contributions of the same order of magnitude. Finally, with electron-electron hole (second diagram (17) and neutron-neutron hole (first diagram (17)) correlations included we recover this statement and the numerical estimate of Voskresensky & Senatorov (1987), Schaab et al. (1997).

Work of Kolomeitsev & Voskresensky (1999) gives another example demonstrating that, although the vacuum branching ratio of the kaon decays is $\Gamma(K^- \rightarrow e^- + \nu_e)/\Gamma(K^- \rightarrow \mu^- + \nu_\mu) \approx 2.5 \times 10^{-5}$, in medium (due to the lambda-proton hole, Λp^{-1} , decays of virtual K^-) it becomes of the order of unity. Thus we again see that depending what reaction channel is considered, in-medium effects may significantly enhance the reaction rates or substantially suppress them. Ignoring these effects may lead to quite misleading results.

2.4. Inconsistencies of the FOPE model

Since the FOPE model is the basis of the “standard” scenario for cooling simulations, which is still in use, we would like to demonstrate inconsistencies in the model for the description of interactions in dense ($n \gtrsim n_0$) baryon medium (see Voskresensky & Senatorov 1986; Voskresensky 2001).

The only diagram in the FOPE model which contributes to the MU and NB is



Dots symbolize FOPE. This is the first available Born approximation diagram, i.e. the second order perturbative contribution in $f_{\pi N}$ coupling. In order to be theoretically consistent one should use perturbation theory up to the same second order in $f_{\pi N}$ for all the quantities. The pion spectrum is then determined by a pion polarization operator expanded up to the same order in $f_{\pi N}$:

$$\omega^2 \simeq m_\pi^2 + k^2 + \Pi_0^R(\omega, k, n), \quad (19)$$

$$\Pi_0^R(\omega, k, n) = \dots \text{ (diagram) } \dots$$

The value $\Pi_0^R(\omega, k, n)$ is easily calculated containing no uncertain parameters. For $\omega \rightarrow 0$, $k \simeq p_F$ and for isospin symmetric matter

$$\begin{aligned} \Pi_0^R &\simeq -\alpha_0 - i\beta_0\omega, \\ \alpha_0 &\simeq \frac{2m_N p_F k^2 f_{\pi N}^2}{\pi^2} > 0, \quad \beta_0 \simeq \frac{m_N^2 k f_{\pi N}^2}{\pi} > 0. \end{aligned} \quad (20)$$

Replacing this value in (19) we obtain a solution $i\beta_0\omega \simeq (\omega^*)^2(k)$ with $\text{Im } \omega < 0$ (for $k \simeq k_m$) already for $n > 0.3n_0$ that would mean appearance of pion condensation ($(\omega^*)^2(k_m) < 0$). Indeed, the mean field begins to grow as $\varphi \sim \exp(-\text{Im } \omega \cdot t) \sim \exp(\alpha t)$, $\alpha > 0$, until repulsive $\pi\pi$ interaction does not stop its growth. But it is experimentally proven that there is no pion condensation in atomic nuclei, i.e. even at $n = n_0$.

The puzzle is solved as follows. The FOPE model does not work for such densities. One should replace FOPE by the full NN interaction given by (4), (7). The essential part of this interaction is due to MOPE with vertices corrected by NN correlations, see (12). Also the particle-hole, NN^{-1} , part of the pion polarization operator is corrected by NN correlations. Thus

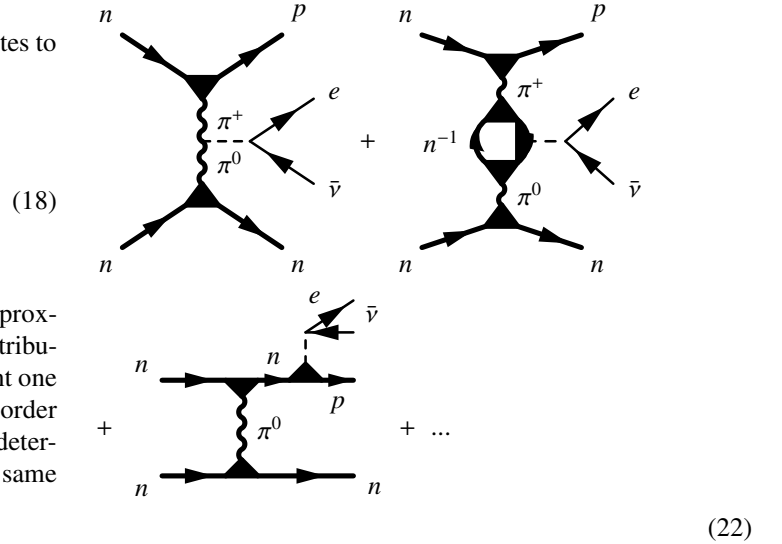
$$\text{(diagram)} \simeq \Pi_0^R(\omega, k, n)\gamma(g', \omega, k, n) \quad (21)$$

is suppressed by the factor $\gamma(g', \omega = 0, k \simeq p_F, n \simeq n_0) \simeq 0.35 \div 0.45$. The final solution of the dispersion relation (19), now with full Π instead of Π_0^R , yields $\text{Im } \omega > 0$ for $n = n_0$ whereas the solution with $\text{Im } \omega < 0$, which shows the beginning of pion condensation, appears only for $n > n_{c\pi} > n_0$.

3. Medium effects in neutrino radiation processes

3.1. Medium effects in two-nucleon processes

Medium effects essentially modify the contributions of all processes. The main contributing diagrams are



It was shown in Voskresensky & Senatorov (1984, 1986, 1987) and Migdal et al. (1990), see also a more recent review Voskresensky (2001), that the main contribution to the MMU process actually comes from the *pion channel* of the reaction $nn \rightarrow npe\bar{\nu}$ (the first diagram in (22)), where $e\bar{\nu}$ are radiated from the intermediate pion exchanging nucleons. Less contribution comes from the NN^{-1} intermediate reaction states (second diagram), and only much less contribution for $n \gtrsim n_0$ comes from the nucleon of the leg of the reaction (third diagram, which naturally generalizes the corresponding MU(FOPE) contribution (18)).

Moreover, due to the *pion softening* (medium modification of the pion propagator) the matrix elements of the MMU process are further enhanced with the increase of the density towards the pion condensation critical point, see Fig. 1. Roughly, the emissivity of MMU reaction then acquires a factor (mainly due to the pion decay channel of MMU)

$$\frac{\varepsilon_\nu[\text{MMU}]}{\varepsilon_\nu[\text{MU}]} \sim 10^3 (n/n_0)^{10/3} \frac{\Gamma^6(n)}{[\omega^*(n)/m_\pi]^8}, \quad (23)$$

where the pre-factor $(n/n_0)^{10/3}$ arises from the phase space volume.

A different enhancement factor arises for the MNB processes, where radiation from intermediate reaction states (see first two diagrams in (22)) is forbidden:

$$\frac{\varepsilon_\nu[\text{MNB}]}{\varepsilon_\nu[\text{NB}]} \sim 10^3 (n/n_0)^{4/3} \frac{\Gamma^6(n)}{[\omega^*(n)/m_\pi]^3}.$$

The value ω^* entering Eqs. (23) and (24) is determined by curve 1a for $n < n_{c\pi}$ and by curve 2 for $n > n_{c\pi}$ if a condensate is present. If a condensate is assumed to be absent one should use the continuation 1b of the curve 1a.

3.2. Medium effects in one-nucleon DU-like processes

3.2.1. MNPBF processes

The one-nucleon processes with neutral currents given by the second diagram (16) for $N = (n, p)$ are forbidden at $T > T_{cN}$ by energy-momentum conservation but they can occur at $T < T_{cN}$, where T_{cN} is the critical temperature for the nucleon-nucleon (NN) pairing. Then the necessary energy and momentum can be taken from breaking and formation of the Cooper pair. However they need special techniques to be calculated, see Flowers et al. (1976), Voskresensky & Senatorov (1987). Their calculation is easily done in terms of closed diagrams with normal and anomalous Green functions, see Voskresensky & Senatorov (1987). These diagrams contain only one nucleon loop. It clearly demonstrates that these processes are indeed one-nucleon-like processes rather than two-nucleon NB-like processes, as one sometimes interprets them. Due to the one-nucleon origin there appears a huge (for the gap $\Delta \gtrsim \text{MeV}$) pre-factor $\sim 10^{29}$ in their emissivity, see Eq. (37) below. Also the typical temperature pre-factor $\sim T^7$ following the rough estimate of Flowers et al. (1976) is actually misleading. Instead there is a $\Delta^7(T/\Delta)^{1/2}$ pre-factor.

These processes (MnPBF) $n \rightarrow n\nu\bar{\nu}$ and (MpPBF) $p \rightarrow p\nu\bar{\nu}$ play very important roles in the cooling of superfluid NS, see Voskresensky & Senatorov (1987), Senatorov & Voskresensky (1987), Migdal et al. (1990), Schaab et al. (1997), Blaschke et al. (2004). Due to the full vertices in (16) extra Γ_{w-s}^2 factors appear in the MPBF emissivity. Medium effects are not as important for the $n \rightarrow n\nu\bar{\nu}$ process, changing the emissivity by a factor of the order of one but they increase the emissivity of the $p \rightarrow p\nu\bar{\nu}$ process by two orders of magnitude, see Eq. (17).

3.2.2. Pion and kaon condensate processes

The P wave pion condensate can be of three types: π_s^+ , π^\pm , and π^0 with different values of the critical densities $n_{c\pi} = (n_{c\pi^\pm}, n_{c\pi^\pm}, n_{c\pi^0})$, see Migdal (1978). Thus above the threshold density for the pion condensation of the given type, the neutrino emissivity of the MMU process (22) is to be supplemented by the corresponding PU processes

$$(24) \quad \begin{array}{c} \bar{\nu} \\ \swarrow \\ e \\ \downarrow \\ n \end{array} \begin{array}{c} \swarrow \\ p \\ \downarrow \\ n \end{array} \begin{array}{c} \swarrow \\ \pi_c^- \\ \downarrow \\ \times \end{array} \quad , \quad \begin{array}{c} \bar{\nu} \\ \swarrow \\ e \\ \downarrow \\ n \end{array} \begin{array}{c} \swarrow \\ p \\ \downarrow \\ n \end{array} \begin{array}{c} \swarrow \\ \pi_c^+ \\ \downarrow \\ \times \end{array} \quad , \quad (25) \quad \begin{array}{c} \bar{\nu} \\ \swarrow \\ e \\ \downarrow \\ p \end{array} \begin{array}{c} \swarrow \\ n \\ \downarrow \\ p \end{array} \begin{array}{c} \swarrow \\ \pi_c^0 \\ \downarrow \\ \times \end{array} \quad , \quad \begin{array}{c} \bar{\nu} \\ \swarrow \\ \nu \\ \downarrow \\ n \end{array} \begin{array}{c} \swarrow \\ n \\ \downarrow \\ n \end{array} \begin{array}{c} \swarrow \\ \pi_c^0 \\ \downarrow \\ \times \end{array} \quad \dots$$

The wavy line with the cross is associated with the amplitude of the pion condensate mean field. Contrary to the FOPE model, the MOPE model of Voskresensky & Senatorov (1986) consistently takes into account the pion softening effects for $n < n_{c\pi}$ and both the pion condensation and pion softening effects in presence of the condensate for $n > n_{c\pi}$. As we have mentioned, in our numerical calculations we assume for simplicity that $n_{c\pi} = n_c^{\text{PU}} \simeq 3 n_0$ is the same for neutral and charged condensates. For vertices in (25) we use the values presented above. Thus, emissivities of the PU processes are suppressed by the $\Gamma_s^2 \Gamma_{w-s}^2$ factors. In the case of a weak condensate field for non-superfluid matter all processes with charged currents yield contributions to emissivity of the same order of magnitude, whereas processes on neutral currents are significantly suppressed, see Voskresensky & Senatorov (1984), (1986), Leinson (2004).

For $n > n_c^{\text{KU}}$ the kaon condensate processes come into play. The most popular is the idea of the S wave K^- condensation (e.g. see Brown et al. 1988; Tatsumi 1988) which is allowed at $\mu_e > m_{K^-}^*$ ($m_{K^-}^*$ is the effective kaon mass) due to possibility of the reaction $e \rightarrow K^- \nu$. Analogous condition for the pion, $\mu_e > m_\pi^*$ (m_π^* is the effective pion mass) is not fulfilled due to a strong S wave πNN repulsion, cf. Migdal (1978), Migdal et al. (1990), (again the in-medium effect), otherwise S wave π^- condensation would occur at lower densities than K^- condensation. The neutrino emissivity of the K^- condensate processes is given by the equation analogous to charged pions however with a different NN correlation factor and an additional suppression factor due to a small contribution of the Cabibbo angle.

The phase structure of dense NS matter might be very rich, including π^0 , π^\pm condensates and \bar{K}^0 , K^- condensates in both S and P waves, see Kolomeitsev & Voskresensky (2003); coupling of condensates, see Umeda et al. (1994); charged ρ -meson condensation, see Voskresensky (1997), Kolomeitsev & Voskresensky (2004); fermion condensation yielding an efficient DU-like process in the vicinity of the pion condensation point (with the emissivity $\varepsilon_\nu \sim 10^{27} T_9^5 m_N^* \propto 1/T$),

see Voskresensky et al. (2000); hyperonization, see Takatsuka & Tamagaki (2004); quark matter with different phases, such as 2SC, CFL, CSL, plus their interaction with meson condensates, see Rajagopal & Wilczek (2000), Blaschke et al. (2001), Grigorian et al. (2004) and refs therein; and different mixed phases. In the present work, as in Blaschke et al. (2004), we suppress all these possibilities of extra efficient cooling channels except a PU process on the pion condensate. Other choices are effectively simulated by our PU choice.

3.2.3. Other resonance processes

There are many other reaction channels allowed in the medium. Any Fermi liquid permits propagation of zero sound excitations of different symmetry related to the pion and the quanta of a more local interaction determined via Landau-Migdal parameters $f_{\alpha\beta}$ and $g_{\alpha\beta}$. These excitations present at $T \neq 0$ may also participate in the neutrino reactions. The most essential contribution comes from the neutral current processes, see Voskresensky & Senatorov (1986), given by the first two diagrams of the series

$$\dots + \dots \quad + \quad \dots + \dots \quad + \dots \quad (26)$$

Here the dotted line is the zero sound quantum of the appropriate symmetry. These are the resonance processes (second one of the DU-type) analogous to those processes on the condensates with the only difference that the rates of reactions with zero sounds are proportional to the thermal occupations of the corresponding spectrum branches whereas the rates of the condensate processes are proportional to the modulus squared of the condensate mean field. The contribution of the resonance reactions is rather small due to the small phase space volume ($q \sim T$) associated with zero sounds. Note the analogy of the processes (26) with the corresponding phonon processes in the crust.

3.2.4. DU processes

The proper DU processes in matter, as $n \rightarrow pe^- \bar{\nu}_e$ and $pe^- \rightarrow n\nu_e$,

$$\dots + \dots \quad + \quad \dots + \dots \quad (27)$$

should also be treated with the full vertices. They are forbidden up to the density n_c^{DU} when the triangle inequality $p_{Fn} < p_{Fp} + p_{Fe}$ begins to be fulfilled. For traditional EoS like that given by the variational theory by Akmal et al. (1998), DU processes are permitted only for $n > 5n_0$. Due to the full vertices in (27) extra Γ_{w-s}^2 factors appear in the DU emissivity.

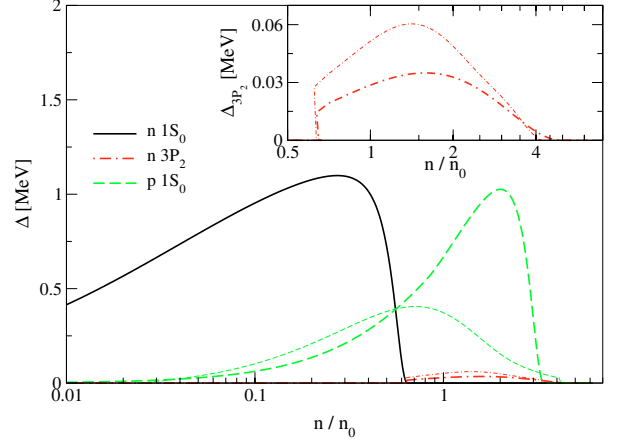


Fig. 2. Neutron and proton pairing gaps according to model I (thick solid, dashed and dotted lines) and according to model II (thin lines), see text. The $1S_0$ neutron gap is the same in both models, taken from Ainsworth et al. (1989).

4. Gaps

In spite of the many calculations that have been performed, the values of nucleon gaps in dense NS matter are poorly known. This is the consequence of the exponential dependence of the gaps on the density dependent potential of the in-medium NN interaction. This potential is not sufficiently well known. Gaps that we have adopted in the framework of the “nuclear medium cooling” scenario, see Blaschke et al. (2004), are presented in Fig. 2. Thick dashed lines show proton gaps used in the work of Yakovlev et al. (2004a) performed in the framework of the “standard plus exotics” scenario. In their model, proton gaps are artificially enhanced (that is, not supported by any microscopic calculations) to get a better fit of the data. We use their “1p” model. Neutron $3P_2$ gaps presented in Fig. 2 (thick dash-dotted lines) are the same as those of the “3nt” model of Yakovlev et al. (2004a). We will call this model I. Thin lines show $1S_0$ proton and $3P_2$ neutron gaps from Takatsuka & Tamagaki (2004), for the model AV18 by Wiringa et al. (1995) (we call it model II). We take the same $1S_0$ neutron gap in both models I and II (thick solid line), as calculated by Ainsworth et al. (1989) and used by Schaab et al. (1997) within the cooling code. Blaschke et al. (2004) used both models I and II within the “nuclear medium cooling” scenario. Since the $1S_0$ neutron pairing gap exists only within the crust, dying for baryon densities $n \geq 0.6n_0$, its effect on the cooling is rather minor. The effect on the cooling arising from the proton $1S_0$ pairing and from the neutron $3P_2$ pairing, with gaps reaching up to rather high densities, is pronounced. The NS cooling essentially depends on the values of the gaps and on their density dependence. Findings of Schulze et al. (1996) and Lombardo & Schulze (2000), who incorporated in-medium effects, motivated us to check the possibility of a suppression of $1S_0$ neutron and proton gaps. For that we introduced pre-factors for $1S_0$ neutron and proton gaps which we varied in the range $0.2 \div 1$, see Figs. 18 and 19 of Blaschke et al. (2004).

4.1. Possibilities either of strong suppression or strong enhancement of $3P_2$ gap

Recently Schwenk & Friman (2004) have argued for a strong suppression of the $3P_2$ neutron gaps, down to values $\lesssim 10$ keV, as a consequence of the medium-induced spin-orbit interaction. They included important medium effects, such as the modification of the effective interaction of particles at the Fermi surface owing to polarization contributions, with particular attention to spin-dependent forces. In addition to the standard spin-spin, tensor and spin-orbit forces, spin non-conserving effective interactions were induced by screening in the particle-hole channels. Furthermore a novel long-wavelength tensor force was generated. The polarization contributions were computed to second order in the low-momentum interaction $V_{\text{low}k}$. These findings motivated Blaschke et al. (2004) to suppress values of $3P_2$ gaps shown in Fig. 2 by an extra factor $f(3P_2, n) = 0.1$. Further possible suppression of the $3P_2$ gap is almost not reflected in the behavior of the cooling curves.

Contrary to expectations of Schwenk & Friman (2004), the more recent work of Khodel et al. (2004) argued that the $3P_2$ neutron pairing gap should be dramatically enhanced, as a consequence of the strong softening of the pion propagator. According to their estimation, the $3P_2$ neutron pairing gap is as large as $1 \div 10$ MeV in a broad region of densities, see Fig. 1 of their work.

In order to apply these results to a broad density interval both models may need further improvement. The model of Schwenk & Friman (2004) was developed to describe not too high densities. It does not incorporate higher order nucleon-nucleon hole loops and the Δ isobar contributions and thus it may only partially include the pion softening effect at densities $\gtrsim n_0$. The model of Khodel et al. (2004) uses a simplified analytic expression for the effective pion gap $(\omega^*)^2(k_m)$, valid near the pion condensation critical point, if the latter occurred by a second order phase transition. The latter assumption means that $(\omega^*)^2(k_m)$ is assumed to be zero in the critical point of the phase transition. Outside the vicinity of the critical point the parameterization of the effective pion gap that was used can be considered only as a rough interpolation. Actually the phase transition is of first order and evaluations of quantum fluctuations done by Dyugaev (1982) show that the value of the jump of the effective pion gap in the critical point is not as small. Moreover repulsive correlation contributions to the NN amplitude have been disregarded. In the pairing channel under consideration, already outside the narrow vicinity of the pion condensation critical point, the repulsion originating from the NN correlation effects may exceed the attraction originating from the pion softening. Notice that, if the pairing gap enhancement occurred only in a rather narrow vicinity of the pion condensation critical point, it would not affect the results of Blaschke et al. (2004). In the latter work two possibilities were considered (see Fig. 1): i) a saturation of the pion softening with increase of the baryon density resulting in the absence of pion condensation and ii) a stronger pion softening stimulating the occurrence of the pion condensation for $n > n_c \approx 3 n_0$. In both cases the effective pion gap was assumed never to

approach zero and undergoing a not too small jump at the critical point from a finite positive value $((\omega^*)^2 \approx 0.3 m_\pi^2)$ to a finite negative value $((\omega^*)^2 \approx -0.1 m_\pi^2)$. The reason for such a strong jump is the strong coupling. If it were so, the strong softening assumed by Khodel et al. (2004) would not be realized. However, due to uncertainties in the knowledge of forces acting in strong interacting nuclear matter and a poor description of the vicinity of the phase transition point we cannot exclude that the alternative possibility of a tiny jump of the pion gap exists. Therefore we will check how these alternative hypotheses may work within our “nuclear medium cooling” scenario. Avoiding further discussion of the theoretical background of the models, we investigate the possibility of a significantly enhanced $3P_2$ neutron pairing gap and of a partially suppressed proton $1S_0$ gap, as suggested by Khodel et al. (2004). To proceed in the framework of our “nuclear medium cooling” scenario we introduce the enhancement factor of the original $3P_2$ neutron pairing gap $f(3P_2, n)$, and a suppression factor of the proton $1S_0$ gap $f(1S_0, p)$. We do not change the neutron $1S_0$ gap since its effect on the cooling is minor.

4.2. Suppression of the emissivity by superfluid gaps

Generally speaking, the suppression factors of superfluid processes are given by complicated integrals. As was demonstrated by Sedrakian (2005) with the example of the DU process, these integrals are not reduced to the R -factors, see Yakovlev et al. (2004a). However, for temperatures significantly below the critical temperature the problem is simplified. With an exponential accuracy the suppression of the specific heat is governed by the factor ξ_{nn} for neutrons and ξ_{pp} for protons:

$$\xi_{ii} \approx \exp[-\Delta_{ii}(T)/T], \quad \text{for } T < T_{ci}; \quad i = n, p, \quad (28)$$

and $\xi_{ii} = 1$ for $T > T_{ci}$, T_{ci} is the corresponding critical temperature. We do not need higher accuracy to demonstrate our result. Therefore we will use these simplified factors.

For the emissivity of the DU process the suppression factor is given by $\min\{\xi_{nn}, \xi_{pp}\}$, see Lattimer et al (1991). The same suppression factor appears for other one nucleon processes, as PU and KU and the resonance processes on zero sounds, see the second diagram of (26). Suppression factors for two nucleon processes follow from this fact and from the diagrammatic representation of different processes within the closed diagram technique by Voskresensky & Senatorov (1987) and Knoll & Voskresensky (1995, 1996). These are: $\xi_{nn} \cdot \min\{\xi_{nn}, \xi_{pp}\}$ for the neutron branch of the MU process (and for the same branch of the medium modified Urca process, MMU); $\xi_{pp} \cdot \min\{\xi_{nn}, \xi_{pp}\}$ for the corresponding proton branch of the process; ξ_{nn}^2 for the neutron branch of the (medium modified) nucleon bremsstrahlung (MnB) and ξ_{pp}^2 for the corresponding proton branch of the bremsstrahlung (MpB). Thus, for $\Delta_{nn} \gg \Delta_{pp}$ both neutron and proton branches of the MMU process are frozen for $T \ll T_{cn}$ due to the factors ξ_{nn}^2 and $\xi_{pp}\xi_{nn}$, respectively. Zero sound and other phonon processes shown by the first diagram (26) are not suppressed by the ξ_{ii} factors. However their contribution to the emissivity is very small due to the smallness of the available phase space volume.

5. Cooling model of Blaschke et al. (2004)

5.1. EoS and structure of NS interior, crust, surface

5.1.1. NS interior

We will exploit the EoS of Akmal et al. (1998) (specifically the Argonne $V18 + \delta v + UIX^*$ model), which is based on the most recent models for the NN interaction with the inclusion of a parameterized three-body force and relativistic boost corrections. Actually we adopt a simple analytic parameterization of this model given by Heiselberg & Hjorth-Jensen (1999) (HHJ). It uses the compressional part with the compressibility $K \simeq 240$ MeV, and a symmetry energy fitted to the data around the nuclear saturation density, and smoothly incorporates causality at high densities. The density dependence of the symmetry energy is very important since it determines the value of the threshold density for the DU process. The HHJ EoS fits the symmetry energy to the original Argonne $V18 + \delta v + UIX^*$ model yielding $n_c^{DU} \simeq 5.19 n_0$ ($M_c^{DU} \simeq 1.839 M_\odot$). The original Argonne EoS allows for neutral pion condensation (for $n > 2n_0$) that only slightly affects the energy density. One may disregard this small change. This EoS does not allow for charged pion condensation. The HHJ parameterization of the EoS does not include π condensation effects. We further assume that pion condensation (neutral and charged) occurs for $n > 3n_0$, see discussion in Blaschke et al. (2004). We assume a minor effect of the pion condensation on the EoS and disregard it. We also disregard changes of the isotopic composition due to the charged pion condensation. The latter effect would be small only if the charged pion condensate field were rather weak. Thus we assume that the HHJ parameterization of the EoS includes both mentioned effects or that they are negligible.

5.1.2. NS crust

The density $n \sim 0.5 \div 0.7 n_0$ is the boundary of the NS interior and the inner crust. In the latter there occurs the so-called “pasta phase” discussed by Ravenhall et al. (1983), see also Maruyama et al. (2005b). Then there is the outer crust and the envelope. Note that our code generates a temperature profile that inhomogeneous during the first $10^2 \div 10^3$ y. The influence of the crust on the cooling and heat transport is minor due to its rather low mass content. Therefore the temperature also changes slightly in the crust up to the envelope.

5.1.3. Envelope

The resulting cooling curves depend on the $T_{in} - T_s$ relation between internal and surface temperatures in the envelope. Figure 3 shows uncertainties existing in this relation. A calculation is presented for the canonical NS: $M = 1.4 M_\odot$, $R = 10$ km with the crust model HZ90 of Yakovlev et al. (2004b). Below we will show that a minimal discrepancy of the increased gap scenario with the data is obtained with what we called “our fit” model in Blaschke et al. (2004). Using other choices like the “Tsuruta law” ($T_s^{Tsur} = (10T_{in})^{2/3}$, where T_s and T_{in} are measured in K) only increases the discrepancy. To compare results with “our fit” model we use the upper boundary curve,

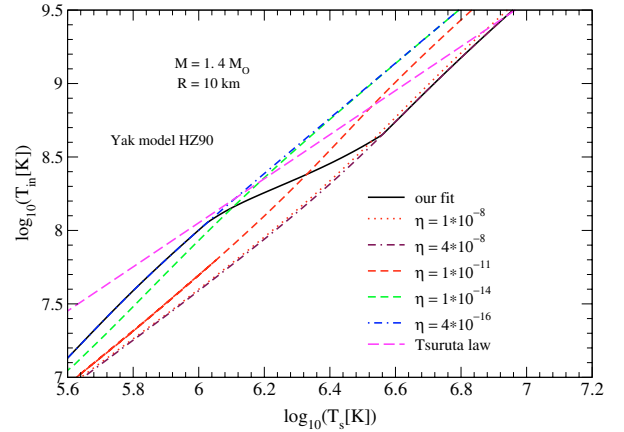


Fig. 3. The relation between the inner crust temperature and the surface temperature for different models. Dash-dotted curves indicate boundaries of the uncertainty band. Notations of lines are determined in the legend. For more details see Blaschke et al. (2004) and Yakovlev et al. (2004b).

$\eta = 4 \times 10^{-16}$ and the lower boundary curve $\eta = 4 \times 10^{-8}$. In Fig. 3 we also draw lines $\eta = 1 \times 10^{-14}$ and $\eta = 1 \times 10^{-11}$ as they are indicated in the corresponding Fig. 2 of Yakovlev et al. (2004b). The selection of $\eta = 4 \times 10^{-8}$ and $\eta = 4 \times 10^{-16}$ as the boundaries of the uncertainty-band seems to be a too strong restriction, see Yakovlev et al. (2004b). The limit of the most massive helium layer is achieved for $\eta \sim 10^{-10}$. On the other hand the helium layer begins to affect the thermal structure only for $\eta > 10^{-13}$. Thus one could exploit $10^{-13} < \eta < 10^{-10}$ as a $T_{in} - T_s$ band. We will use a broader band, as is shown in Fig. 3. By this we simulate the effect of maximum uncertainties in the knowledge of the $T_{in} - T_s$ relation.

5.2. Main cooling regulators

We compute the NS thermal evolution adopting our fully general relativistic evolutionary code. This code was originally constructed for the description of hybrid stars by Blaschke et al. (2001). The main cooling regulators are the thermal conductivity, the heat capacity and the emissivity. In order to better compare our results with results of other groups we try to be as close as possible to their inputs for the quantities that we did not calculate ourselves. Then we add the changes, improving the EoS and including the medium effects.

5.2.1. Thermal conductivity

We take the electron-electron contribution to the thermal conductivity and the electron-proton contribution for normal protons from Gnedin & Yakovlev (1995). The total contribution related to electrons is then given by

$$1/\kappa_e = 1/\kappa_{ee} + 1/\kappa_{ep}. \quad (29)$$

For $T > T_{cp}$ (normal “n” matter), we have $\kappa_{ep}^n = \kappa_{ep}$. For $T < T_{cp}$ (superfluid “s” matter) we use the expression

$$\kappa_{ep}^s = \kappa_{ep}/\xi_{pp} > \kappa_{ep}^n, \quad (30)$$

that gives a crossover from the non-superfluid case to the superfluid case. The vanishing of κ_{ep}^s for $T \ll T_{cp}$ is a consequence of the scattering of superfluid protons on the electron impurities, see Blaschke et al. (2001). Following (29) we get $\kappa_e^n < \kappa_e^s$.

For the neutron contribution,

$$\kappa_n = 1/\kappa_{nn} + 1/\kappa_{np}, \quad (31)$$

we use the result of Baiko et al. (2001) that includes corrections due to the superfluidity. Although some medium effects are incorporated in this work, the nucleon-hole corrections of correlation terms and the modification of the tensor force are not included. This should modify the result. However, since we did not calculate κ_n ourselves, we can only roughly estimate the modification: not too close to the critical point of the pion condensation the squared matrix element of the NN interaction $|M|_{\text{med}}^2 \sim p_{F,n}^2 \Gamma_s^2 / (\omega^*)^2$, see Eq. (12) and values shown in Fig. 1, is of the order of the corresponding quantity $|M|_{\text{vac}}^2 \sim p_{F,n}^2 / [m_\pi^2 + p_{F,n}^2]$ estimated with the free one pion exchange, whereas $|M|_{\text{med}}^2$ may significantly increase for $n \sim n_c^{\text{PU}}$. However Blaschke et al. (2004) checked that both increasing and decreasing of the thermal conductivity does not change the picture as a whole.

The proton term is calculated similarly to the neutron one,

$$\kappa_p = 1/\kappa_{pp} + 1/\kappa_{np}. \quad (32)$$

The total thermal conductivity is the sum of the partial contributions

$$\kappa_{\text{tot}} = \kappa_e + \kappa_n + \kappa_p + \dots \quad (33)$$

For the values of the gaps used in Blaschke et al. (2004) the other contributions to this sum are smaller than those presented explicitly (κ_e , κ_n and κ_p). Finally Blaschke et al. (2004) concluded that in their scenario transport is relevant only up to the first 10^3 y.

5.2.2. Heat capacity

The heat capacity contains nucleon, electron, photon, phonon and other contributions. The main in-medium modification of the nucleon heat capacity is due to the density dependence of the effective nucleon mass. We use the same expressions as Schaab et al. (1997). The main regulators are the nucleon and the electron contributions. For the nucleons ($i = n, p$), the specific heat is (Maxwell 1979)

$$c_i \sim 10^{20} (m_i^*/m_N) (n_i/n_0)^{1/3} \xi_{ii} T_9 \text{ erg cm}^{-3} \text{ K}^{-1}, \quad (34)$$

for the electrons it is

$$c_e \sim 6 \times 10^{19} (n_e/n_0)^{2/3} T_9 \text{ erg cm}^{-3} \text{ K}^{-1}. \quad (35)$$

Near the phase transition point the heat capacity acquires a pion fluctuation contribution. For the first order pion condensation phase transition this additional contribution contains no singularity, like for the second order phase transition, see Voskresensky & Mishustin (1982) and Migdal et al. (1990). Finally, the nucleon contribution to the heat capacity may increase up to several times in the vicinity of the pion condensation point. The effect of this correction on global cooling properties is unimportant and simplifying we neglect it.

The symmetry of the $3P_2$ superfluid phase allows for the contribution of Goldstone bosons (phonons):

$$C_G \simeq 6 \times 10^{14} T_9^3 \frac{\text{erg}}{\text{cm}^3 \text{ K}}, \quad (36)$$

for $T < T_{cn}(3P_2)$, $n > n_{cn}(3P_2)$. We include this term in our study although its effect on the cooling is minor. A similar contribution comes from other resonance processes permitted on zero sounds, see the first diagram in (26). In order not to introduce an extra parameter dependence we will simulate the effect of all phonon and zero sound terms with the term (36).

5.2.3. Emissivity

We adopt the same set of partial emissivities as in the work of Schaab et al. (1997). The phonon contribution to the emissivity of the $3P_2$ superfluid phase, as well as the zero sound contribution, is negligible. The main emissivity regulators are the MMU, see the rough estimation (23), MnPBF and MpPBF, and MNB processes. For $n > n_c^{\text{PU}} \simeq 3 n_0$ the PU process becomes efficient and for $n > n_c^{\text{DU}} \simeq 5.19 n_0$ the DU process is the dominant.

Only the qualitative behavior of the interaction shown in Fig. 1 is motivated by the microscopic analysis whereas the actual numerical values of the correlation parameter and the pion gap are rather uncertain. Thus we vary the values $\Gamma(n)$ and $\omega^{*2}(n)$ in accordance with the discussion of Fig. 1. By that we check the relevance of alternative possibilities: a) no pion condensation and a saturation of the pion softening with increasing density, curves 1a + 1b, and b) the presence of pion condensation, curves 1a + 2 + 3. We also add the contribution of the DU for $n > n_c^{\text{DU}}$.

All emissivities are corrected by correlation effects. The PU process contains an extra Γ_s^2 factor compared to the DU process (the emissivity of the latter is $\propto \Gamma_{w-s}^2$). Another suppression of PU emissivity comes from the fact that it is proportional to the squared pion condensate mean field $|\varphi|^2$. Near the critical point $|\varphi|^2 \sim 0.1$, increasing with density up to $|\varphi|^2 \sim f_\pi^2/2$, where $f_\pi \simeq 93$ MeV is the pion decay constant. Finally, the PU emissivity is suppressed by about 1–2 orders of magnitude compared to the DU one. We adopt the same gap dependence for the PU process as for the corresponding DU process. In superfluid matter all emissivity terms are suppressed by the corresponding ξ_{ii} factors.

6. Main cooling regulators in the scenario of Khodel et al. (2004)

When neutron processes are frozen the most efficient process is the MpPBF process, $p \rightarrow pv\bar{\nu}$, for $T < T_{cp}$. Taking into account the medium effects in the weak coupling vertex, see Eq. (17), we use the same expression for the emissivity of this process as has been used by Voskresensky (2001) and Blaschke et al. (2004):

$$\begin{aligned} \varepsilon_\nu[\text{MpPBF}] &\sim 10^{29} \frac{m_N^*}{m_N} \left[\frac{p_{Fp}}{p_{Fn}(n_0)} \right] \left[\frac{\Delta_{pp}}{\text{MeV}} \right]^7 \\ &\times \left[\frac{T}{\Delta_{pp}} \right]^{1/2} \xi_{pp}^2 \frac{\text{erg}}{\text{cm}^3 \text{ s}}, \quad T < T_{cp}. \end{aligned} \quad (37)$$

This process contributes only below the critical temperature for proton pairing. Inclusion of medium effects greatly enhances the vertex of this process compared to the vacuum vertex, see the above discussion of this fact in Sect. 2.3. A factor $\Gamma_{w-s}^2 \sim 10^2$ arises, since the process may occur through nn^{-1} and ee^{-1} correlation states, with subsequent production of $\nu\bar{\nu}$ from the $nn^{-1}\nu\bar{\nu}$ and $ee^{-1}\nu\bar{\nu}$ channels rather than from a strongly suppressed channel $pp^{-1}\nu\bar{\nu}$, see Voskresensky & Senatorov (1987), Senatorov & Voskresensky (1987), Migdal et al. (1990), Voskresensky et al. (1998), Leinson (2000) and Voskresensky (2001). Relativistic corrections incorporated in the description of the $pp^{-1}\nu\bar{\nu}$ vertex in Yakovlev et al. (2004a) also produce an enhancement being however significantly less than that arises from medium effects in $nn^{-1}\nu\bar{\nu}$ and $ee^{-1}\nu\bar{\nu}$ channels. Thus we see no reason not to include these medium effects and we note only a moderate dependence of the result on the uncertainties in the strong interaction.

We also present here an explicit expression for the emissivity of the proton branch of the nucleon bremsstrahlung including medium effects, MpB, $pp \rightarrow pp\nu\bar{\nu}$. In the case of suppressed neutron $3P_2$ gaps this process contributes much less than the nucleon bremsstrahlung processes involving neutrons. However, when neutron reactions are frozen, the $pp \rightarrow pp\nu\bar{\nu}$ process becomes the dominating process for $T_{cn} > T > T_{cp}$. The emissivity of the $pp \rightarrow pp\nu\bar{\nu}$ reaction takes the form, see Voskresensky & Senatorov (1986) for more details,

$$\epsilon(\text{MpB}) \sim 10^{23} \zeta_{pp}^2 I_{pp} \frac{Y_p^{5/3} \Gamma_s^4 T_9^8}{(\omega^*)^4 (k_m)} \times \left(\frac{m_p^*}{m_N} \right)^4 \left(\frac{n}{n_0} \right)^{5/3} \frac{\text{erg}}{\text{cm}^3 \text{ s}}, \quad (38)$$

$T_9 = T/10^9$ K, m_p^* is the effective proton mass. Here we take $\Gamma_s \simeq \Gamma(n) \simeq 1/[1 + C(n/n_0)^{1/3}]$, $C \simeq 1.4 \div 1.6$. This factor takes into account NN correlations in strong interaction vertices, $Y_p = n_p/n$ is the proton to nucleon ratio. As above, for simplicity we assumed that the value $k = k_m$ (at which the square of the effective pion gap $(\omega^*)^2(k)$ is minimum) is rather close to the value of the neutron Fermi momentum p_{Fn} , as it follows from the microscopic analysis of Migdal et al. (1990). To simplify the consideration we take the same value of the effective pion gap for the given process as that for the MMU process (although in general it is not so, and thus the result (38) is model dependent), cf. Blaschke et al. (2004),

$$I_{pp} \sim \frac{\pi}{64} \left(\frac{p_{Fn}}{p_{Fp}} \right)^5 \frac{\omega^*(k_m)}{p_{Fn}}. \quad (39)$$

We have checked that for $T < T_{cp}$ for the pairing gaps under consideration the MpB reaction contributes significantly less than the MpPBF process. It could be not the case only in a narrow vicinity of the pion condensation critical point, if pion condensation occurred with only a tiny jump of the effective pion gap in the critical point. However, even in this case there are many effects which could mask this abnormal enhancement.

For $n > n_c^{\text{PU}}$ the process $p\pi_c^0 \rightarrow p\nu\bar{\nu}$ on the neutral pion condensate is still permitted. However its contribution is strongly suppressed, see Leinson (2004).

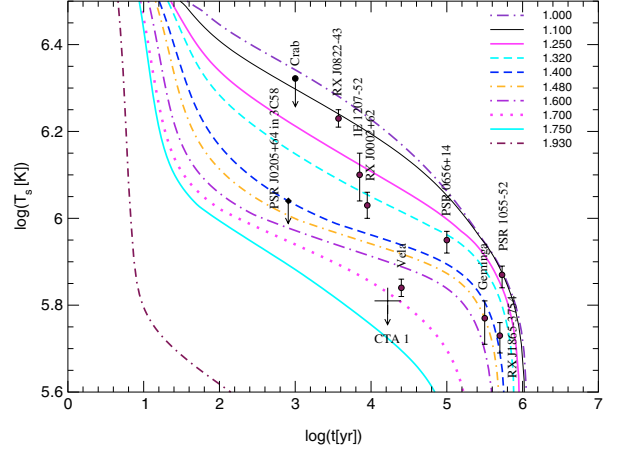


Fig. 4. Figure 21 of Blaschke et al. (2004). Gaps are from Fig. 2 for model II. The original $3P_2$ neutron pairing gap is additionally suppressed by the factor $f(3P_2, n) = 0.1$. The pion gap is determined by curves $1a+2+3$ of Fig. 1. The $T_s - T_{in}$ relation is given by “our fit” curve of Fig. 3. Here and in all subsequent figures the value T_s is the red-shifted temperature. NS masses are indicated in the legend; see Blaschke et al. (2004).

In the case of frozen neutron degrees of freedom the specific heat is governed by protons and electrons, see Eq. (34) for $i = p$ and (35). Here, we again suppress the contribution to the specific heat by the narrow vicinity of the pion condensation critical point due to the fact that in our scenario (see Fig. 1) the modulus of the squared effective pion gap $(\omega^*)^2$ is always larger than $\sim(0.1 \div 0.3) m_\pi^2$. With such an effective pion gap the pion contribution to the specific heat is not as strong and can be disregarded to simplify the consideration. For the second order phase transition (and for a first order phase transition but with a tiny jump of $|(\omega^*)^2|$ in the critical point), pion fluctuations would contribute more strongly to the specific heat yielding a term $c_\pi \propto T_c^{\text{PU}}/\omega^*$ for $|T - T_c^{\text{PU}}|/T_c^{\text{PU}} \ll T_c^{\text{PU}}$, see Voskresensky & Mishustin (1982), Migdal et al. (1990).

When neutron processes are frozen the values κ_n and κ_p are suppressed and the thermal conductivity is reduced to the electron and proton contributions, see Eqs. (29) and (32).

7. Numerical results

Now we give the results of our calculations of cooling curves. First we present Fig. 21 of Blaschke et al. (2004), now Fig. 4. Cooling curves shown in this figure were calculated using “our fit” model of the crust, shown with the solid curve in Fig. 3. Here and in the corresponding figures below the surface temperature is assumed to be red-shifted, as observed at infinity from the radiation spectrum. Gaps are given by model II of Fig. 2. However, the $3P_2$ gap is additionally suppressed by a factor $f(3P_2, n) = 0.1$, as motivated by calculations of Schwenk & Friman (2004). The calculation includes pion condensation for $n > n_c^{\text{PU}}$. The figure shows a good fit to the data. If we used calculations disregarding the possibility of pion condensation (see curves $1a + 1b$ of Fig. 1) we would also get an appropriate fit to the data, cf. Fig. 20 of Blaschke et al. (2004). If we took the original $3P_2$ gap of model II, we would not be

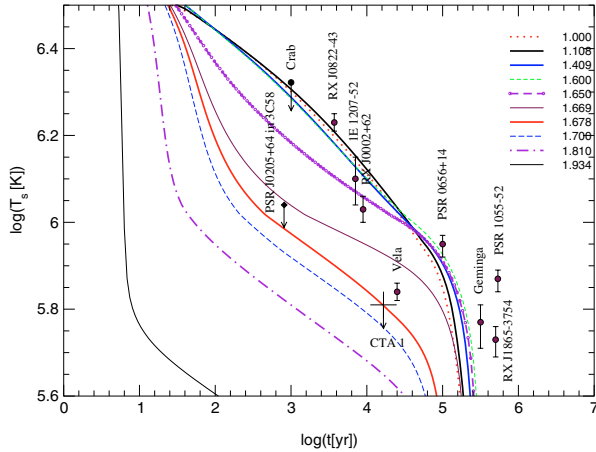


Fig. 5. Cooling curves according to the nuclear medium cooling scenario, see Fig. 4. Gaps are from Fig. 2 for model II but the $3P_2$ neutron pairing gap is additionally enhanced by a factor $f(3P_2, n) = 50$ and the $1S_0$ proton gap is suppressed by $f(1S_0, p) = 0.1$. The pion gap is determined by curves 1a+2+3 of Fig. 1. The $T_s - T_{in}$ relation is given by “our fit” curve of Fig. 3.

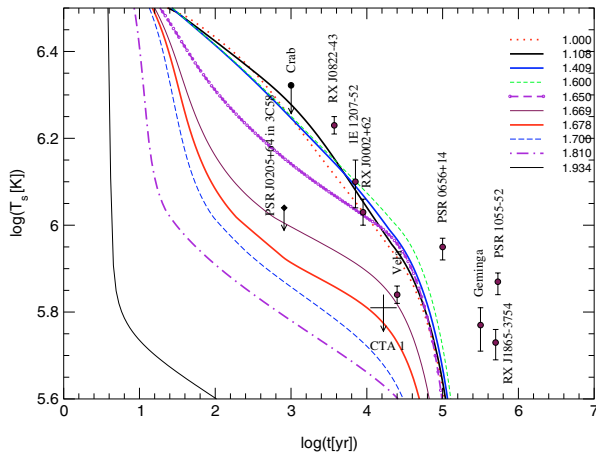


Fig. 6. Same as Fig. 5, but for the original $1S_0$ proton gap suppressed by $f(1S_0, p) = 0.5$.

able to describe the data. The cooling would be too fast, see Fig. 23 of Blaschke et al. (2004).

We will now check the possibility of ultra-high $3P_2$ neutron pairing gaps, as proposed by Khodel et al. (2004). In Figs. 5 and 6 we demonstrate the sensitivity of the results presented in Fig. 4 to the enhancement of the neutron $3P_2$ gap and to a suppression of the $1S_0$ proton gap, following the suggestion of Khodel et al. (2004). Again we use the calculation including pion condensation for $n > n_c^{PU}$.

We start with “our crust” model and model II for the gaps, using however the additional enhancement factor $f(3P_2, n) = 50$ for the neutron $3P_2$ gap. Introducing factors $f(1S_0, p) = 0.1$ and $f(1S_0, p) = 0.5$ we test the sensitivity of the results to the variation of the $1S_0$ proton gap. We do not change the value of the $1S_0$ neutron gap since its variation almost does not influence on the cooling curves for NSs with masses $M > 1 M_\odot$, that we will consider.

Comparison of Figs. 4–6 shows that in all cases NSs with masses $M \gtrsim 1.8 M_\odot$ cool in similar ways in spite of the fact

that $3P_2$ neutron and $1S_0$ proton gaps vary over wide limits. This is because $3P_2$ neutron and $1S_0$ proton gaps disappear at the high densities occurring in the central regions of these very massive NSs, see Fig. 2. Thus these objects cool similarly to non-superfluid objects. Extremely rapid cooling of stars with $M \geq 1.84 M_\odot$ is due to the DU process, which is very efficient in normal matter. The latter process appears in the central region of NSs with $M > 1.839 M_\odot$. Therefore we notice that *the cooling curves are very sensitive to the density dependence of the gaps*. The difference in the cooling of NSs with $M < 1.8 M_\odot$ in the cases presented in Figs. 5 and 6 is the consequence of different values of proton gaps used in these two calculations. This difference is mainly due to the MpPBF processes. The larger the proton gap, the more rapid is the cooling.

We checked that for stars with $M \lesssim 1.6 M_\odot$ for $T < T_{cn}$ for the $3P_2$ neutron pairing, a complete freezing of the neutron degrees of freedom occurs for $f(3P_2, n) \gtrsim 20$. Then contributions to the emissivity and to the specific heat involving neutrons are fully suppressed. For heavier stars ($M > 1.6 M_\odot$) a weak dependence on the value of the factor $f(3P_2, n)$ still remains even for $f(3P_2, n) > 100$ but the corresponding cooling curves lie too low to allow for an appropriate fit of the data. This difference between cooling of stars with $M < 1.6 M_\odot$ and $M > (1.6 \div 1.7) M_\odot$ is due to the mentioned density dependence of the neutron $3P_2$ gap. The latter value smoothly decreases with the increase of the density reaching zero for $n \gtrsim 4.5 n_0$ (the density $4.5 n_0$ is achieved in the center of a NS of mass $M = 1.7 M_\odot$). At densities slightly below $4.5 n_0$ the gap is small. Therefore for stars with $M > (1.6 \div 1.7) M_\odot$ the scaling of the gap by a factor $f(3P_2, n)$ changes the size of the region where the gaps may affect the cooling. For stars with $M \lesssim 1.6 M_\odot$ gaps have finite values even at the center of the star. Thus there exists a critical value of the factor $f(3P_2, n)$, such that for higher values of $f(3P_2, n)$ the cooling curves are unaffected by its change.

Figures 5 and 6 demonstrate that we did not succeed in reaching an appropriate overall agreement with the data; the cooling was too rapid. The cooling of old pulsars is not explained in all cases. Although the heating mechanism used by Tsuruta (2004) may partially help in this respect, the discrepancy between the curves and the data points seems to be too high, especially in Fig. 6. We see that in our regime of frozen neutron processes a better fit is achieved in Fig. 5, i.e., for a stronger suppressed proton gap (for $f(1S_0, p) = 0.1$). The discrepancy is even more severe, since to justify the idea of Khodel et al. (2004) we should use a softer pion propagator. Only a strong softening of the pion mode might be consistent with a significant increase of the neutron $3P_2$ gap. On the other hand such an additional softening would result in still more rapid cooling. The work of Voskresensky et al. (2000) discussed the possibility of a novel very efficient process with the emissivity $\epsilon_v \propto T^5$, that would occur due to non-Fermi liquid behavior of the Fermi sea very near the pion condensation critical point with the assumption of strong pion softening. If we included this very efficient process, the disagreement with the data could be strongly enhanced. An enhancement of the specific heat due to pion fluctuations within the vicinity of the pion condensation point cannot compensate for the acceleration of

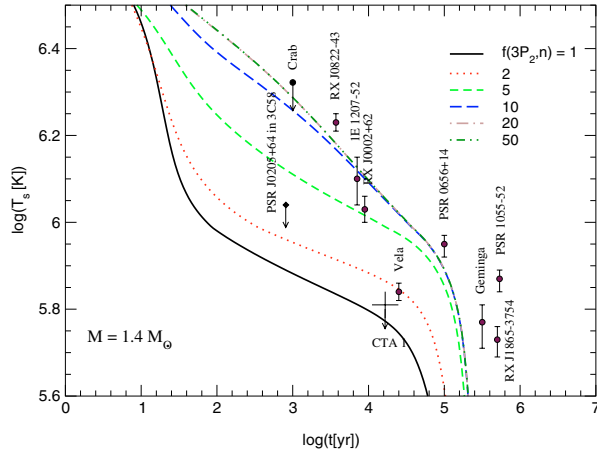


Fig. 7. Cooling curves of the neutron star with mass $1.4 M_{\odot}$ according to the nuclear medium cooling scenario, see Fig. 4. Gaps are from Fig. 2 for model II but the $3P_2$ neutron pairing gap is additionally enhanced by different factors $f(3P_2, n)$ (shown in figure) and the $1S_0$ proton gap is suppressed by $f(1S_0, p) = 0.1$. The pion gap is determined by curves $1a+2+3$ of Fig. 1. The $T_s - T_{in}$ relation is given by “our fit” curve of Fig. 3.

the cooling owing to the enhancement of the emissivity. Khodel et al. (2004) used the value $n_c = 2 n_0$ for the critical density of the pion condensation. In case of the Urbana-Argonne equation of state that we exploit here (we use the HHJ fit of this equation of state that removes the causality problem, see Blaschke et al. (2004) for details) the density $n = 2 n_0$ is achieved in the central region of a NS with the mass $M \sim 0.8 M_{\odot}$. This means that all NSs with $M \geq 0.8 M_{\odot}$ would cool extremely fast and would not be seen in soft X rays.

Actually, we checked the whole interval of variation of $f(3P_2, n)$ and $f(1S_0, p)$ in the range $1 \div 100$ and $0.1 \div 0.5$ respectively. We verified that the variation of $f(3P_2, n)$ and $f(1S_0, p)$ in the whole mentioned range done within our parameterization of the effective pion gap does not improve the picture (curves $1a + 2 + 3$ of Fig. 1). Using the pion gap from branches $1a + 1b$ does not achieve a better fit. In all cases we obtain too rapid cooling. To demonstrate this, in Fig. 7 we show the cooling of a $1.4 M_{\odot}$ star for different values of the $f(3P_2, n)$ factor. The factor $f(1S_0, p)$ is taken to be 0.1. We see that for $f(3P_2, n) < 15 \div 20$ the curves rise with the increase of $f(3P_2, n)$. For $f(3P_2, n) > 20$ the curves do not depend on $f(3P_2, n)$.

To check how the results are sensitive to uncertainties in our knowledge of the value (39) that determines the strength of the in-medium effect on the emissivity of the MpB process we multiplied (38) by a pre-factor $f(\text{MpB})$ that we varied in the range $f(\text{MpB}) = 0.2 \div 5$. In agreement with the above discussion, for $f(\text{MpB}) < 1$, for temperatures $\log T_s[\text{K}] > 5.9$ the cooling curves are shifted upwards. For $f(\text{MpB}) > 1$, for temperatures $\log T_s[\text{K}] > 5.9$ the cooling curves are shifted downwards. However, independently of the value $f(\text{MpB})$ for $\log T_s[\text{K}] < 5.9$ the curves are not changed. Thus it does not allow us to diminish the discrepancy with the data.

Now we will check the efficiency of another choice of the gaps, as motivated by model I, thick lines in Fig. 2. Compared

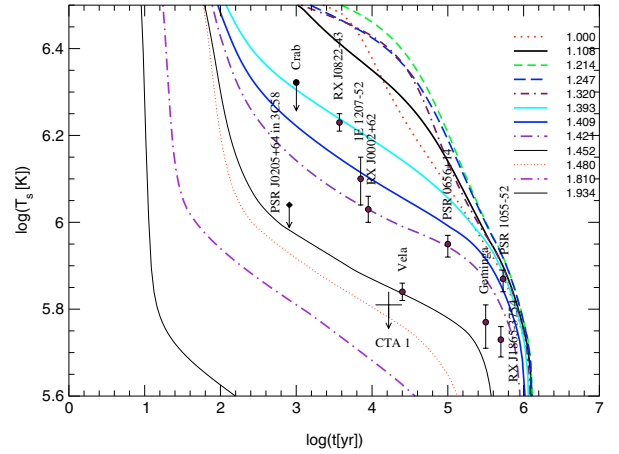


Fig. 8. Figure 15 of Blaschke et al. (2004). Gaps from model I. The original $3P_2$ neutron gap is suppressed by $f(3P_2, n) = 0.1$. The pion gap is determined by curves $1a+2+3$ of Fig. 1. The $T_s - T_{in}$ relation is given by “our fit” curve of Fig. 3. For more details see Blaschke et al. (2004).

to model II model I uses an *artificially enhanced proton gap*. Thus, one can expect that model I is less realistic than model II. Also note a different density dependence of the proton gaps in model I (it cuts off at densities $n \geq 3.2 n_0$) and in model II (it cuts off at higher densities, $n \geq 4.2 n_0$). Since uncertainties in the existing calculations of the gaps are very high and the parameterization of model I has been used by one of the groups working on the problem of cooling of NSs, see Yakovlev et al. (2004a), we will consider the consequences of this possibility as well.

Figure 8 demonstrates our previous fit of the data within model I, but for the original $3P_2$ neutron gap suppressed by $f(3P_2, n) = 0.1$, see Blaschke et al. (2004). Again the pion gap is determined by curves $1a + 2 + 3$ of Fig. 1.

If we took the original $3P_2$ gap of model I, we would not succeed in describing the data. The cooling would be too fast, see Fig. 22 of Blaschke et al. (2004). Therefore we check the possibility of ultra-high $3P_2$ neutron pairing gaps, as proposed by Khodel et al. (2004).

As in Fig. 5, Fig. 9 uses $f(3P_2, n) = 50$ and $f(1S_0, p) = 0.1$ but now for the gap in model I, and, as in Fig. 6, Fig. 10 uses $f(1S_0, p) = 0.5$ for the gap in model I. Figures 9 and 10 show that within the variation of the gaps of model I the discrepancy to the data is still stronger compared to that for the above calculation based on the use of model II. The difference between curves shown in Figs. 9 and 10 is less pronounced than for those curves in Figs. 5 and 6. Indeed, as we have mentioned, the density dependence of the proton gap is different in models I and II. In model II the proton gap reaches higher densities ($\approx 4.2 n_0$) than in model I ($\approx 3.2 n_0$). Thus in the case shown by Figs. 9 and 10 a non-superfluid core begins to contribute at lower values of the star mass. Therefore in both figures the corresponding cooling curves are almost the same for $M \geq 1.6 M_{\odot}$. Using the pion gap from branches $1a + 1b$, i.e. disregarding the possibility of pion condensation, does not allow a better fit.

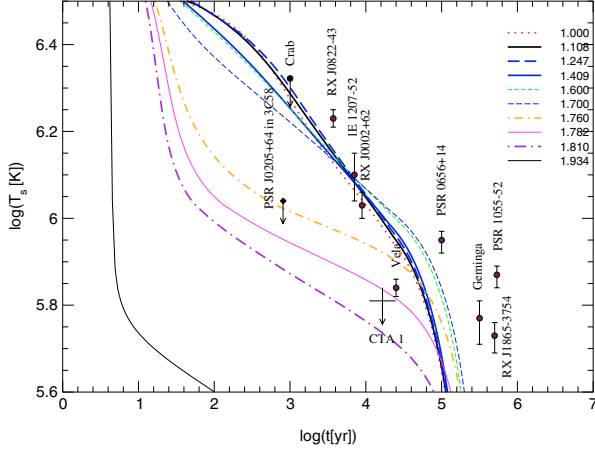


Fig. 9. Cooling curves according to the nuclear medium cooling scenario, see Fig. 8. Gaps are from Fig. 2 for model I but the $3P_2$ neutron pairing gap is additionally enhanced by a factor $f(3P_2, n) = 50$ and the $1S_0$ proton gap is suppressed by $f(1S_0, p) = 0.1$. The pion gap is determined by curves $1a+2+3$ of Fig. 1. The $T_s - T_{in}$ relation is given by “our fit” curve of Fig. 3.

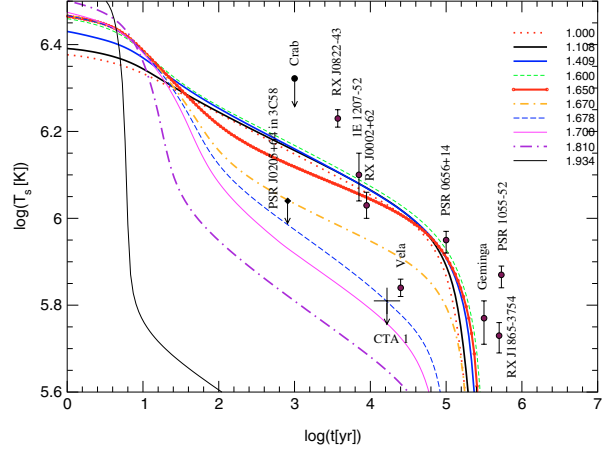


Fig. 11. Cooling curves according to the nuclear medium cooling scenario. Gaps are from Fig. 2 for model II but the $3P_2$ neutron pairing gap is additionally enhanced by a factor $f(3P_2, n) = 50$ and the $1S_0$ proton gap is suppressed by $f(1S_0, p) = 0.1$. The pion gap is determined by curves $1a+2+3$ of Fig. 1. The $T_s - T_{in}$ relation is given by the crust model for $\eta = 4.0 \times 10^{-16}$.

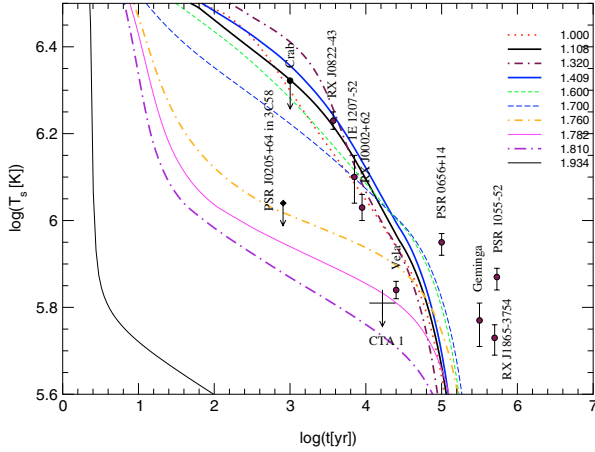


Fig. 10. Same as Fig. 9, but for the original $1S_0$ proton gap suppressed by $f(1S_0, p) = 0.5$.

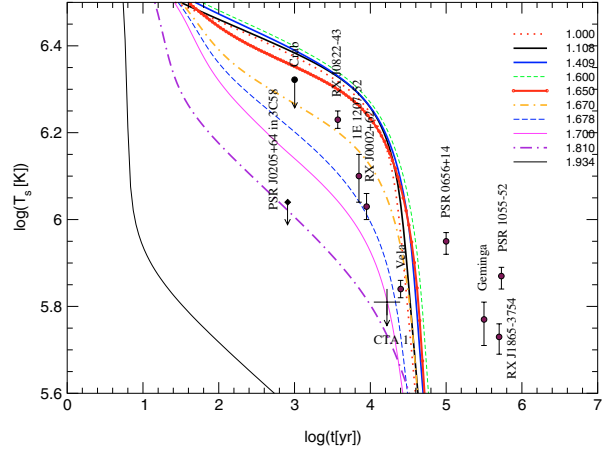


Fig. 12. Same as in Fig. 11, but for the crust model $\eta = 4.0 \times 10^{-8}$.

The dependence of the results on the different choices of the $T_s - T_{in}$ relation is demonstrated by Figs. 11 and 12 for gaps based on a modification of model II. For this demonstration we first took the upper boundary curve $\eta = 4 \times 10^{-16}$ and then the lower boundary curve $\eta = 4.0 \times 10^{-8}$ in Fig. 3. We show that these choices however do not allow us to improve the fit. Comparing Figs. 11 ($\eta = 4 \times 10^{-16}$) and 5 (“our fit”) based on the same modification of model II we see that with the “our fit” crust model (Fig. 5) the deviation from the data points is less pronounced. We have checked that based on model I one arrives at the same conclusion. An increase of the factor $f(1S_0, p)$ to 0.5 reduces the fit. In Fig. 12 we use the lower boundary curve $\eta = 4.0 \times 10^{-8}$ of Fig. 3. We further demonstrate that the selection of a different choice of the $T_s - T_{in}$ relation within the band shown in Fig. 3 does not diminish the discrepancy. This discrepancy increases compared to that demonstrated by “our fit” model. Indeed, the cooling evolution for times $t \lesssim 10^5$ yr ($T_s \gtrsim 10^6$ K) is governed by neutrino processes. Thus the higher T_{in} , the larger T_s is. The

slowest cooling is then obtained, if one uses the lower boundary curve $\eta = 4.0 \times 10^{-8}$ of Fig. 3. The evolution of NSs for times $t \gtrsim 10^5$ yr begins to be controlled by the photon processes. In the photon epoch ($t \gg 10^5$ yr) the smaller the T_s value, the less efficient the radiation is. Thus for $t \gg 10^5$ yr the slowest cooling is obtained if one uses the upper boundary curve $\eta = 4.0 \times 10^{-16}$ of Fig. 3. The “our crust” curve simulates the transition from one limiting curve to the other demonstrating the slowest cooling in the temperature interval shown in the figures.

In all cases the data are not explained by the assumption of an enhanced neutron $3P_2$ gap (for $f(3P_2, n) > 1$) and a partially suppressed $1S_0$ proton gap (for $f(1S_0, p) = 0.1 \div 0.5$).

8. Concluding remarks

Our aim was to consider large $3P_2$ gaps within the “nuclear medium cooling” scenario of Blaschke et al. (2004) that well described the cooling data with the opposite assumption of suppressed $3P_2$ gaps. Therefore we did not incorporate extra

assumptions of internal heating for old pulsars, see Tsuruta (2004), and quark cores in massive NSs, see Blaschke et al. (2001) and Grigorian et al. (2004) and refs therein.

The main problem with the given scenario is that at the frozen neutron contribution to the specific heat and to the emissivity, the region of surface temperatures $T_s > 10^6\text{K}$ is determined by proton processes. The most efficient among them is the MpPBF process for $T < T_{cp}$ and MpB for $T > T_{cp}$. For the proton gaps that we deal with, the MpPBF process proves to be too efficient, yielding too rapid cooling. Thus at least several slow cooling data points (at least in data for old pulsars) are not explained. Some works ignore the medium-induced enhancement of the MpPBF emissivity that results in a 10–100 times suppression of the rate. We omitted this possibility as physically unrealistic. The origin of this enhancement is associated with opening up of new reaction channels in the medium that are forbidden in vacuum.

Thus, we have shown that the “nuclear medium cooling” scenario of Blaschke et al. (2004) fails to appropriately fit the neutron star cooling data with the assumption of a strong enhancement of the $3P_2$ neutron gaps (we checked the range $f(3P_2, n) = 1 \div 100$) and for moderately suppressed $1S_0$ proton gaps (for $f(1S_0, p) = 0.1 \div 0.5$). On the other hand the same scenario allowed us to appropriately fit the whole set of data with the assumption of a significantly suppressed $3P_2$ neutron gap (for $f(3P_2, n) \sim 0.1$). We observed essential dependence of the results not only on the values of the gaps but also on their density dependence. We used the density dependence of the gaps according to models I and II. The latter model is supported by microscopic calculations. We excluded an attempt to artificially fit the density dependence of the gaps trying to match cooling curves with the data. Although such an attempt could improve the fit, it is not physical and we did not pursue it. However we encourage further attempts of microscopic calculations of the gaps, which would take into account the most important medium effects. With correctly treated gaps one could perform new simulations of NS cooling.

Acknowledgements. We thank D. Blaschke for his interest in our work, critical reading of the manuscript and valuable remarks. We also thank B. Friman and A. Schwenk for interesting discussions and A.Y. Potechin for helpful comments. The research of H.G. was supported by the Virtual Institute of the Helmholtz Association under grant No. VH-VI-041 and by the DAAD partnership program between the Universities of Rostock and Yerevan. The work of D.N.V. was supported in part by the Deutsche Forschungsgemeinschaft (DFG project 436 RUS 113/558/0-2), the Russian Foundation for Basic Research (RFBR grant 03-02-04008) and RF President grant NS-5898.2003.02.

References

Ainsworth, T., Wambach, J., & Pines, D. 1989, Phys. Lett. B, 222, 173
 Akmal, A., Pandharipande, V. R., & Ravenhall, D. G. 1998, Phys. Rev. C, 58, 1804
 Bahcall, J. N., & Wolf, R. A. 1965, Phys. Rev. B, 140, 1445
 Baiko, D. A., Haensel, P., & Yakovlev, D. G. 2001 [arXiv:astro-ph/0105105]

Blaschke, D., Grigorian, H., & Voskresensky, D. N. 2001, A&A, 368, 561
 Blaschke, D., Grigorian, H., & Voskresensky, D. N. 2004, A&A, 424, 979
 Borzov, I. N., Tolokonnikov, S. V., & Fayans, S. A. 1984, Sov. J. Nucl. Phys., 40, 732
 Brown, G. E., Kubodera, K., Page, D., & Pizzochero, P. 1988, Phys. Rev. D, 37, 2042
 Dyugaev, A. M. 1975, Pisma v ZhETF, 22, 181
 Dyugaev, A. M. 1982, JETP Lett., 35, 420
 Fayans, S. A., & Zawischa, D. 1995, Phys. Lett. B, 363, 12
 Flowers, E., Ruderman, M., & Sutherland, P. 1976, ApJ, 205, 541
 Friman, B., & Maxwell, O. V. 1979, ApJ, 232, 541
 Glendenning, N. K. 1992, Phys. Rev., D, 46, 1274
 Gnedin, O. Y., & Yakovlev, D. G. 1995, Nucl. Phys. A, 582, 697
 Grigorian, H., Blaschke, D., & Voskresensky, D. N. 2004, Phys. Rev. C, 71, 045801
 Heiselberg, H., & Hjorth-Jensen, M. 1999 [arXiv:astro-ph/9904214]
 Ivanov, Yu. B., Knoll, J., van Hees, H., & Voskresensky, D. N. 2001, Phys. Atom. Nucl., 64, 652
 Khodel, V. A., Clark, J. W., Takano, M., & Zverev, M. V. 2004, Phys. Rev. Lett. 93, 151101
 Knoll, J., & Voskresensky, D. N. 1995, Phys. Lett. B, 351, 43
 Knoll, J., & Voskresensky, D. N. 1996, Ann. Phys. (N. Y.) 249, 532
 Kolomeitsev, E. E., & Voskresensky, D. N. 1999, Phys. Rev. C, 60, 034610
 Kolomeitsev, E. E., & Voskresensky, D. N. 2003, Phys. Rev. C, 68, 015803
 Kolomeitsev, E. E., & Voskresensky, D. N. 2005, Nucl. Phys. A, 759, 373 [arXiv:nuc1-th/0410063]
 Landau, L. D. 1956, Sov. JETP, 3, 920
 Lattimer, J. M., Pethick, C. J., Prakash, M., & Haensel, P. 1991, Phys. Rev. Lett., 66, 2701
 Leinson, L. B. 2000, Phys. Lett. B, 473, 318
 Leinson, L. B. 2004 [arXiv:astro-ph/0411025]
 Lombardo, U., & Schulze, H.-J. 2001, in Physics of Neutron Stars Interiors, ed. D. Blaschke, N. K. Glendenning, & A. Sedrakian, Lect. Notes Phys., 578, 30
 Maruyama, T., Tatsumi, T., Voskresensky, D. N., Tanigawa, T., & Chiba, S. 2004, AIP Conf. Proc. 7004, 519 [arXiv:nuc1-th/0311076]
 Maruyama, T., Tatsumi, T., Voskresensky, D. N., Tanigawa, T., & Chiba, S. 2005a, Nucl. Phys. A, 749, 186
 Maruyama, T., Tatsumi, T., Voskresensky, D. N., Tanigawa, T., & Chiba, S. 2005b [arXiv:nuc1-th/0502040]
 Maxwell, O. V. 1979, ApJ, 231, 201
 Migdal, A. B. 1967, Theory of Finite Fermi Systems and Properties of Atomic Nuclei (New York: Wiley and Sons; second. ed. (in Rus.), Moscow: Nauka, 1983)
 Migdal, A. B. 1978, Rev. Mod. Phys.: 50, 107
 Migdal, A. B., Saperstein, E. E., Troitsky, M. A., & Voskresensky, D. N. 1990, Phys. Rept., 192, 179
 Page, D., Lattimer, J. M., Prakash, M., & Steiner, A. W. 2004, ApJS, 155, 623
 Rajagopal, K., & Wilczek, F. 2000 [hep-ph/0011333]
 Rapp, R., & Wambach, J. 1994, Nucl. Phys., A, 573, 626
 Ravenhall, D. G., Pethick, C. J., & Wilson, J. R. 1983, Phys. Rev. Lett., 50, 2066
 Saperstein, E. E., & Tolokonnikov, S. V. 1998, JETP Lett., 68, 553
 Schaab, Ch., Voskresensky, D., Sedrakian, A. D., Weber, F., & Weigel, M. K. 1997, A&A, 321, 591
 Schulze, H.-J., Cugnon, J., Lejeune, A., Baldo, M., & Lombardo, U. 1996, Phys. Lett. B, 375, 1

- Schwenk, A., & Friman, B. 2004, *Phys. Rev. Lett.* 92, 082501
- Sedrakian, A. 2005, *Phys. Lett. B.* 607, 27
- Senatorov, A. V., & Voskresensky, D. N. 1987, *Phys. Lett. B.* 184, 119
- Shapiro, S., & Teukolsky, S. A. 1983, *Black Holes, White Dwarfs and Neutron Stars: The Physics of Compact Objects* (New-York, USA: Wiley-Interscience)
- Suzuki, T., Sakai, H., & Tatsumi, T. 1999, [arXiv:nucl-th/9901097]
- Takatsuka, T., & Tamagaki, R. 2004, *Prog. Theor. Phys.*, 112, 37
- Tatsumi, T. 1988, *Prog. Theor. Phys.*, 80, 22
- Tsuruta, S., & Cameron, A. G. W. 1965, *Canad. J. Phys.*, 43, 2056
- Tsuruta, S. 1979, *Phys. Rept.*, 56, 237
- Tsuruta, S. 2004, in *Proc. IAU Symp., Young Neutron Stars and their Environments*, ed. F. Camilo, & B. M. Gaensler, 218 [arXiv:astro-ph/0401245]
- Tsuruta, S., Teter, M. A., Takatsuka, T., Tatsumi, T., & Tamagaki, R. 2002, *ApJ*, 571, L143
- Umeda, H., Nomoto, K., Tsuruta, S., Muto, T., & Tatsumi, T. 1994, *ApJ*, 431, 309
- Voskresensky, D. N. 1997, *Phys. Lett. B.* 392, 262
- Voskresensky, D. N. 2001, in *Physics of Neutron Stars Interiors*, ed. D. Blaschke, N. K. Glendenning, & A. Sedrakian, *Lect. Notes Phys.* 578, 467 [arXiv:astro-ph/0101514]
- Voskresensky, D. N., & Mishustin, I. N. 1981, *JETP Lett.*, 34, 303
- Voskresensky, D. N., & Mishustin, I. N. 1982, *Sov. J. Nucl. Phys.*, 35, 667
- Voskresensky, D. N., & Senatorov, A. V. 1984, *JETP Lett.*, 40, 1212
- Voskresensky, D. N., & Senatorov, A. V. 1986, *JETP*, 63, 885
- Voskresensky, D. N., & Senatorov, A. V. 1987, *Sov. J. Nucl. Phys.*, 45, 411
- Voskresensky, D. N., Kolomeitsev, E. E., & Kämpfer, B. 1998, *JETP*, 87, 211
- Voskresensky, D. N., Khodel, V. A., Zverev, M. V., & Clark, J. W. 2000, *ApJ*, 533, L127
- Voskresensky, D. N., Yasuhira, M., & Tatsumi, T. 2002, *Phys. Lett.*, B, 541, 93
- Voskresensky, D. N., Yasuhira, M., & Tatsumi, T. 2003, *Nucl. Phys. A*, 723, 291
- Wiringa, R. B., Stoks, V. G., & Schiavilla, R. 1995, *Phys. Rev. C*, 51, 38
- Yakovlev, D. G., Gnedin, O. Y., Kaminker, A. D., Levenfish, K. P., & Potekhin, A. Y. 2004a, *Adv. Space Res.*, 33, 523
- Yakovlev, D. G., Levenfish, K. P., Potekhin, A. Y., Gnedin, O. Y., & Chabrier, G. 2004b, *A&A*, 417, 169